Report

"Modeling the Blue-Green Algal Bloom in the Neuse River Estuary"

Submitted to:

The Soap and Detergent Association
475 Park Avenue South at 32nd Street
New York, NY 10016

Attention: Dr. Keith A. Booman
Technical Director

Submitted by:

Wu-Seng Lung
Assistant Professor
Department of Civil Engineering
University of Virginia

and

Hans W. Paerl
Professor
Institute of Marine Sciences
University of North Carolina

Report No. UVA/531076/CE86/101

March 1986

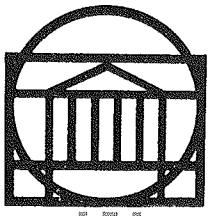

SCHOOL OF ENGINEERING AND
APPLIED SCIENCE

DEPARTMENT OF CIVIL ENGINEERING

UNIVERSITY OF VIRGINIA
CHARLOTTESVILLE, VIRGINIA 22901

Report

"Modeling the Blue-Green Algal Bloom in the Neuse River Estuary"

Submitted to:

The Soap and Detergent Association
475 Park Avenue South at 32nd Street
New York, NY 10016

Attention: Dr. Keith A. Booman
Technical Director

Submitted by:

Wu-Seng Lung
Assistant Professor
Department of Civil Engineering
University of Virginia

and

Hans W. Paerl
Professor
Institute of Marine Sciences
University of North Carolina

Report No. UVA/531076/CE86/101
March 1986

Copy No. _____

TABLE OF CONTENTS

LIST OF TABLES

LIST OF FIGURES

LIST OF FIGURES

ACKNOWLEDGEMENTS

Grateful thanks are due to Dr. Keith A. Booman and Mr. Richard I. Sedlak, Jr. of the Soap and Detergent Association. Their enthusiasm helped to make the conduct of this research most enjoyable.

Special thanks are also due to Ms. Donna L. Richardson and Ms. Audrey L. Shipley of the Department of Civil Engineering, University of Virginia, for their assistance in carrying out the computations. The assistance of Mr. Dean Bowles of the Institute of Marine Sciences, University of North Carolina on compiling the water quality data is also appreciated.

Special thanks are given to Dr. George T. Everett and his staff of the Water Quality Section Division of Environmental Management for providing additional water quality data. Dr. J. Kent Crawford of the USGS in Raleigh has supplied river discharge data for this study.

EXECUTIVE SUMMARY AND CONCLUSIONS

A. Summary

An estuarine eutrophication model has been developed to quantify the blue-green algal blooms in the lower Neuse River, North Carolina. The important features of the model include four functional groups of phytoplankton: diatoms, greens, non-nitrogen fixing blue-greens, and nitrogen fixing blue-greens; a two-layer mass transport pattern in a portion of the estuary; and the effect of salinity on algal growth. In addition, each of the two layers in the water column is divided into longitudinal segments to account for the concentration gradients of the water quality constituents.

The water quality constituents simultaneously simulated by the model are chlorophyll a levels associated with the four algal groups, organic nitrogen, ammonia nitrogen, nitrite and nitrate nitrogen, organic phosphorus, orthophosphate, dissolved oxygen, and salinity. Biochemical, biological, and chemical interactions between the water quality constituents are incorporated into the model to quantify phytoplankton growth and death, algal species competition, nutrient uptake and recycle, and photosynthetic reproduction and respiration consumption of oxygen by algae.

A large data base primarily consisting of the water quality and phytoplankton data (1983 and 1984) from the Institute of Marine Sciences, University of North Carolina was used in the model development, model calibration and sensitivity analyses. Additional data from other studies on the lower Neuse was also used in this modeling study.

The model calibration results for the surface segments under the 1983 condition are summarized in Figure A. The model is able to mimic the trend of the data in 1983 reasonably well. The year 1983 was characterized by high runoff in the spring months and low flow in the summer months. In addition, the water in the Neuse River was warm and calm in the summer of 1983. As a result, significant blue-green algal blooms occurred. Figure B shows the observed and model calculated chlorophyll a concentrations associated with the four algal groups in the lower Neuse in 1983.

The 1984 condition was characterized by a similar magnitude of runoff in the spring months as 1983. However, the summer flow in 1984 was much higher than that in the summer of 1983. As a result, the blue-green bloom did not occur although a modest population of phytoplankton was maintained in 1984 (Figure C).

B. Conclusions

The following conclusions are presented, based on the modeling analysis presented in this study.

1. Based on the model calibration of the 1983 and 1984 data, it is concluded that the initiation and maintenance of the blue-green bloom is strongly regulated by the nutrient supply from the spring months as well as the river flow and the associated hydrodynamic conditions in the summer months. The modeling analysis has confirmed this hypothesis.

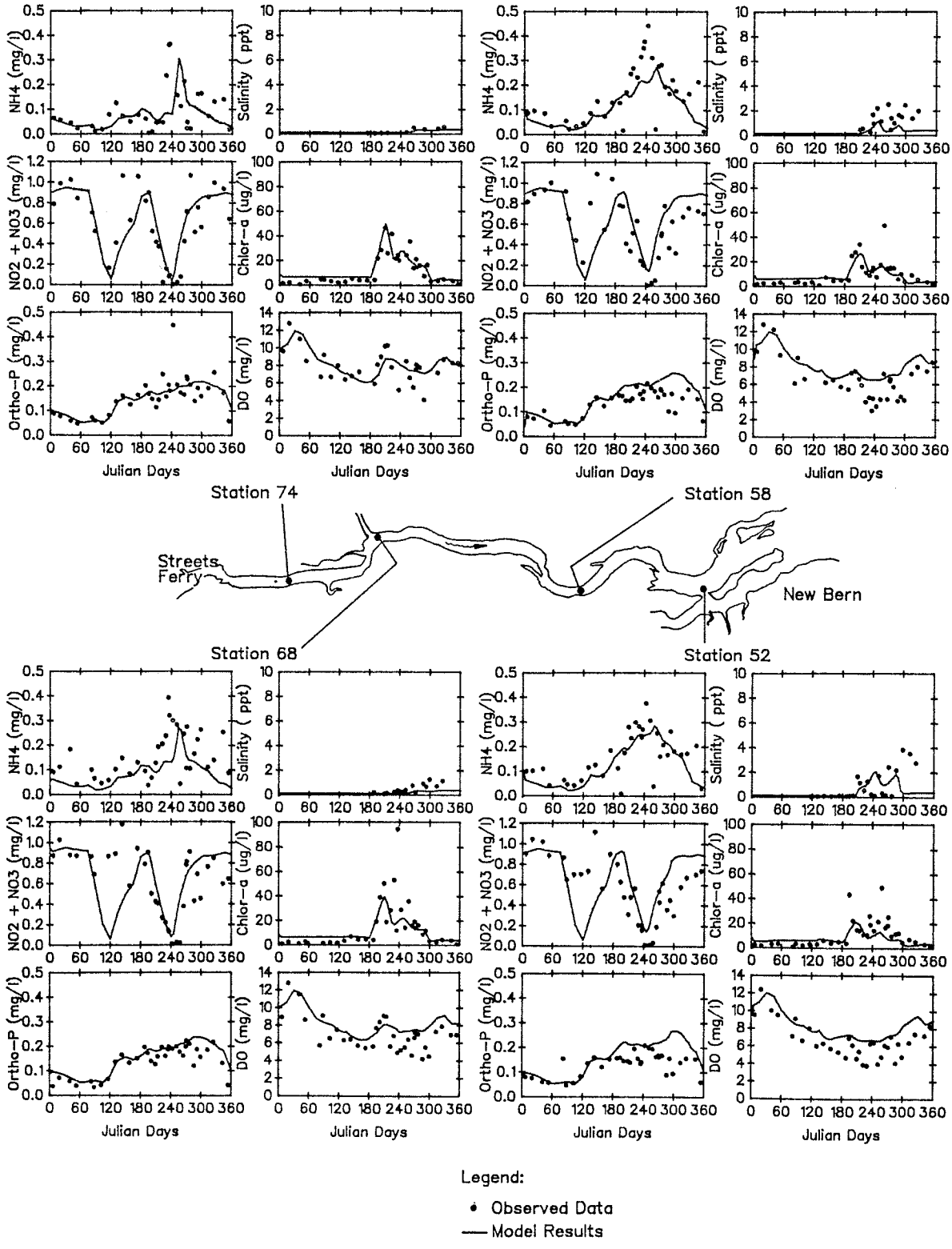

Figure A. Model Calibration of 1983 Data – Neuse River Estuary

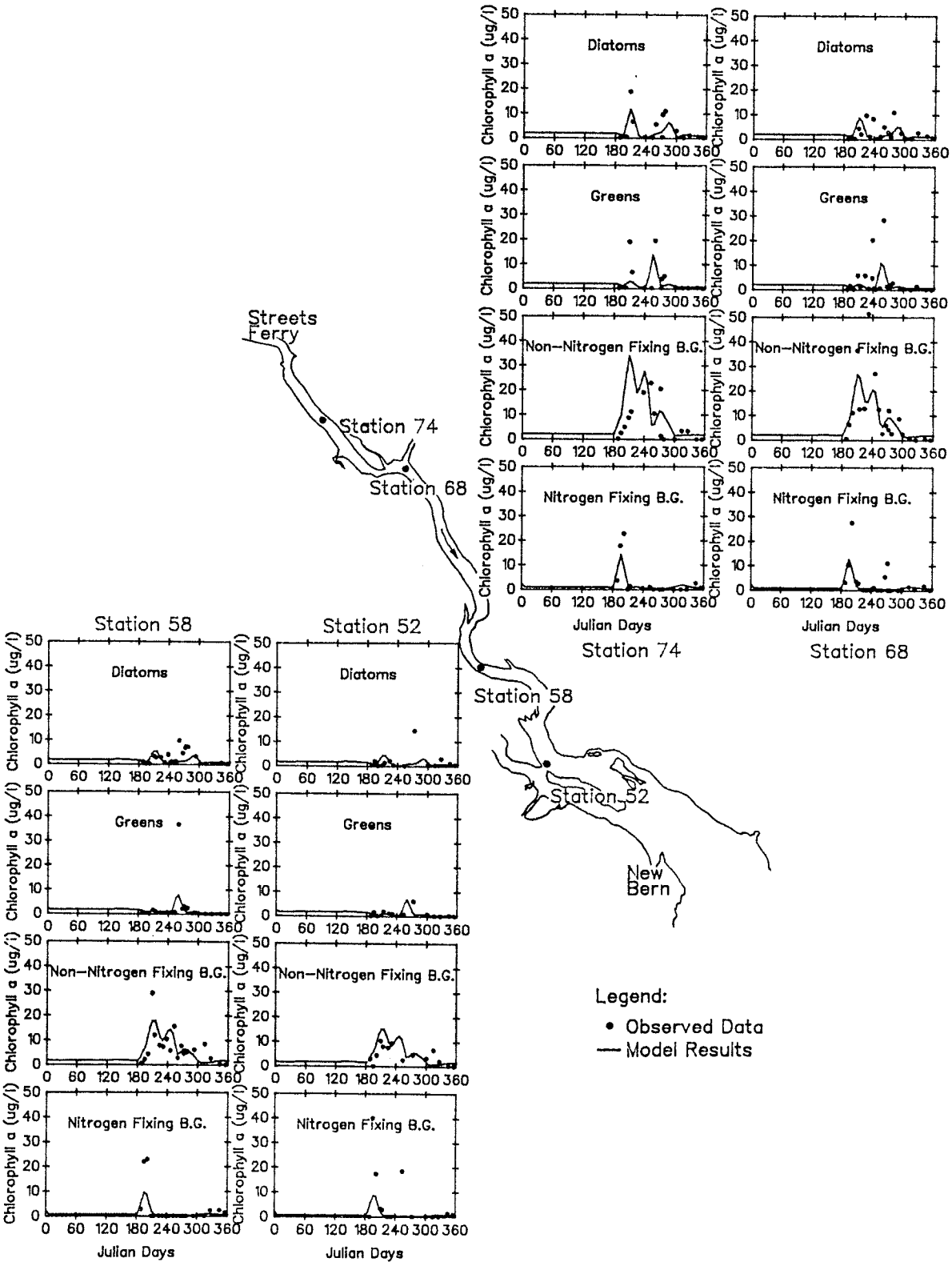

Figure B. Summary of Algal Species Calibration Results, 1983

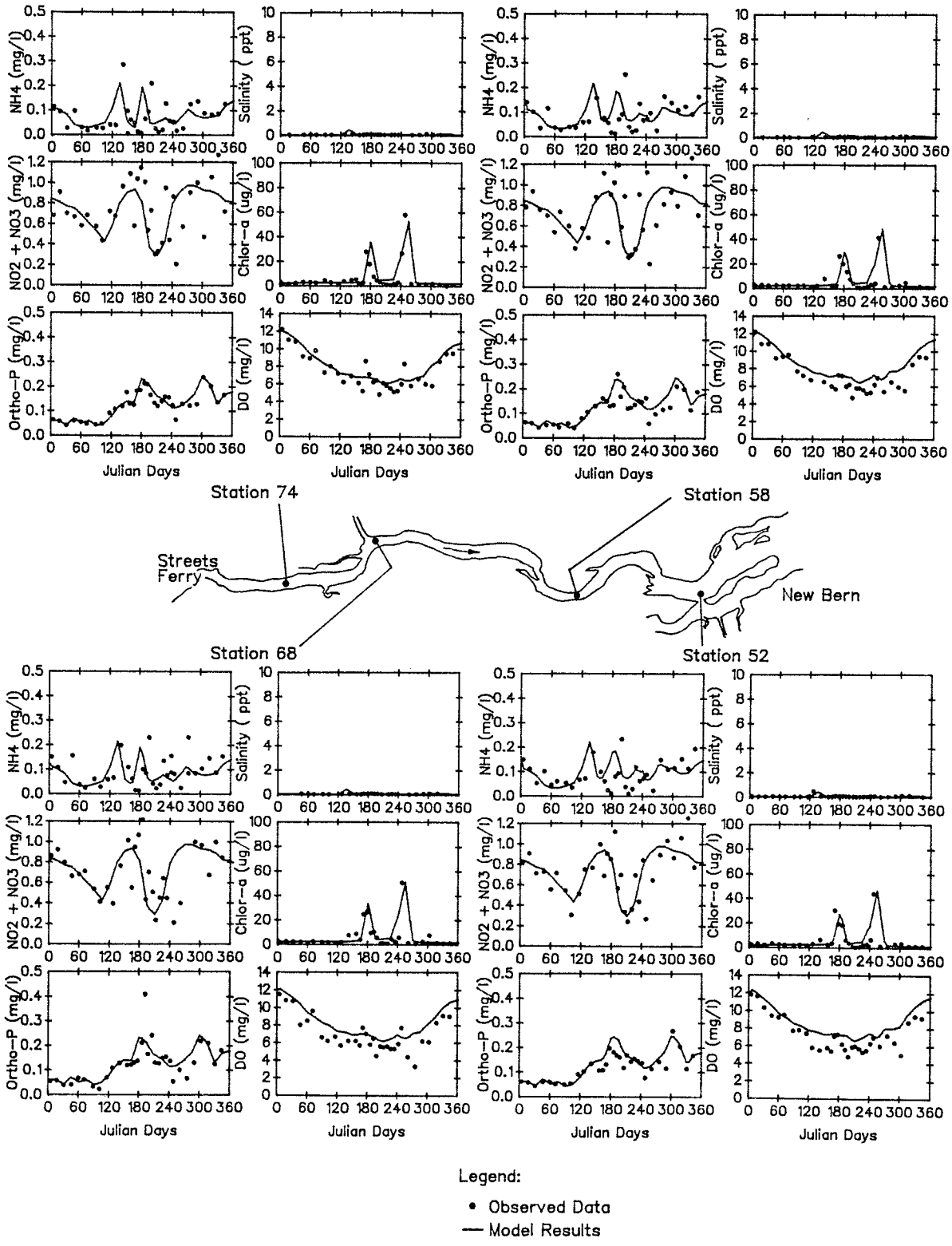

Figure C. Model Calibration of 1984 Data – Neuse River Estuary

2. More specifically , the blue-green algal blooms and their associated growth are influenced by the upstream boundary conditions of the model. Successful modeling of the blue-green blooms would require accurate assignment of the upstream boundary conditions, particularly for projecting the trends of system response under various water quality management schemes.

3. Nutrients (nitrogen and phosphorus) are not limiting factors for the initiation of blooms in the lower Neuse River in 1983 and 1984. However, nitrogen proved limiting in 1983 once the bloom became firmly established. Further, light or turbidity and sudden hydrological changes (flow increases) are the major factors which cause the decline of an existing blue-green bloom.

4. Salinity also plays a role in controlling the algal growth rate. The effect is particularly pronounced during the summer period of low flows because salinity intrusion would reach the bloom area under low flow conditions (i.e., 1983 conditions).

5. Incorporation of sediment nutrient releases and dissolved inorganic carbon as a state variable has been identified as future model enhancement to better address the impact of nutrient control on algal growth.

1. INTRODUCTION AND PURPOSE

Segments of the lower Neuse River between Goldsboro and New Bern, North Carolina (Figure 1) have, over the past decade, revealed alarming symptoms of advanced eutrophication, culminating in the appearance and persistence of nuisance blue-green algal blooms. Specific symptoms of eutrophication in the lower Neuse are (1) generally high rates of primary productivity and standing stocks of algal biomass, often in excess of 25 µg/l chlorophyll a; (2) periodic spring and summer blooms of nuisance blue-green algae, particularly the surface dwelling non-nitrogen fixing colonial species Microcystis aeruginosa; and (3) algal nutrient levels of both nitrogen (ammonia and nitrate) and phosphorus (orthophosphate) greatly exceeding levels which are considered to be growth-limiting to nuisance species at the initiation of blooms (Paerl, 1983).

Concern for mitigative steps being asked from a management perspective include:

- Will major reductions of nutrient (nitrogen and/or phosphorus) inputs (either from point or nonpoint sources) to the lower Neuse River help to control further eutrophication and specifically arrest the occurrence and persistence of nuisance blue-green algal blooms?
- What magnitudes of nitrogen and/or phosphorus input cutbacks are required to control and ultimately eliminate the nusiance blue-green algae bloom potentials on the lower Neuse River?

Before these questions can be answered and any sound water quality management scheme can be implemented, we need to understand the mechanisms initiating and sustaining algal bloom in the lower Neuse

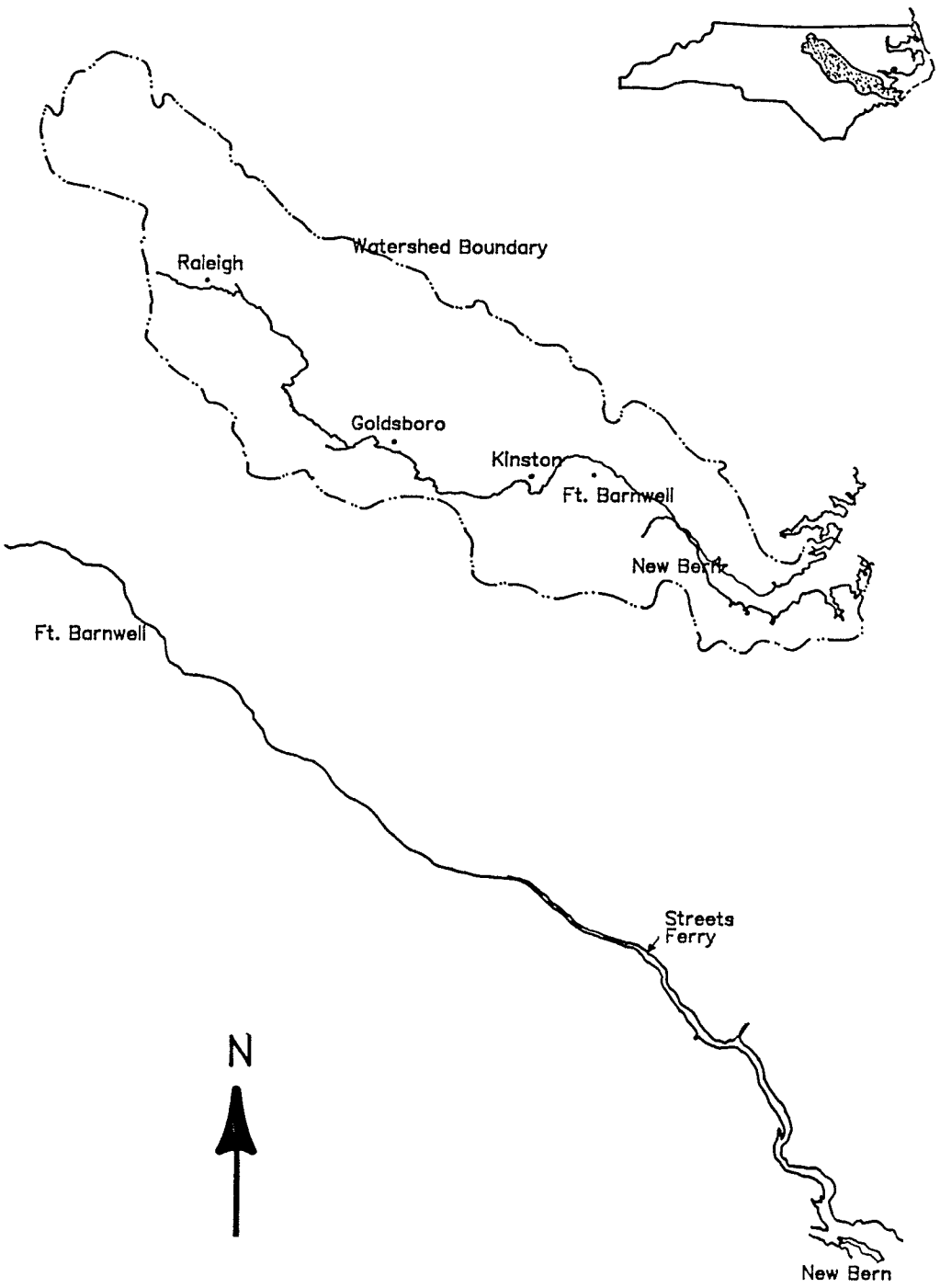

Figure 1. The Neuse River Watershed and the Study Area

River. Although the data from many field studies of the Neuse River has provided some clue as to the nutrient effect on the phytoplankton growth as well as the roles played by other factors regulating the bloom, more or less, on a qualitative basis, there is a pressing need for a quantitative tool to assist decision making for a sound management strategy.

To help address these questions, a mathematical model of the lower Neuse River has been developed. The modeling effort focuses on several key technical areas related to the understanding of the mechanisms initiating and sustaining algal blooms in the lower Neuse River:

- an evaluation and quantification of the environmental (physical, chemical) factors regulating the initiation of the blue-green algae bloom;
- development of a mass transport pattern suitable to address the flow related aspects of the bloom;
- development of a phytoplankton (in four functional groups) model of the lower Neuse River;
- calibration and vertification of the developed models using the 1983 and 1984 data.

The water quality data collected in the past few years by the Institute of Marine Sciences, University of North Carolina were used in the model development. Major features of the model include multiple phytoplankton functional groups such as the diatoms, green algae, blue-greens (nitorgen fixing and non-nitrogen fixing), and salinity effect on the algae growth. In the model, the water column is sliced into two layers to characterize the near surface activities of the

blue-greens (i.e., Microcystis aeruginosa). Important environmental conditions such as light, temperature, and river flow are incorporated into the model.

The results of the modeling study show that the model reproduces the temporal and spatial trends of the 1983 and 1984 data reasonably well. The river flow condition strongly influences the initiation and maintenance of the blue-green blooms. The dominant phytoplankton group is the non-nitrogen fixing blue-green algae, Microcystis aeruginosa. Under low flow conditions, the two-layer mass transport pattern and associated salinity intrusion play a role in controlling the algal growth in the lower Neuse.

2. DATA ANALYSIS

2.1 Sources of Data

Concern about the eutrophication of the lower Neuse River has prompted many research efforts and field investigations (Tedder et al., 1980; Paerl, 1983; Paerl et al., 1984). As a result, there is a good amount of water quality data available for this modeling study. The Institute of Marine Sciences (Morehead City) of the University of North Carolina at Chapel Hill has been collecting the water quality data of the lower Neuse since 1979 (Paerl, 1983; Paerl et al., 1984). In addition, researchers from East Carolina University have also studied the eutrophication of the lower Neuse (Christian and Stanley, 1984; Stanley and Christian, 1984). Additional data was also available from the North Carolina Department of Natural Resources (NCDNR, 1984) and the University of North Carolina Water Resources Research Institute.

2.2 Water Quality Data of 1983

The Institute of Marine Sciences has been collecting the water quality data at a number of stations in the lower Neuse River from Streets Ferry Bridge in Vanceboro to New Bern (see Figure 1) since 1981. The following water quality parameters (from the 1983 data) are presented in Figure 2: dissolved inorganic carbon (DIC), ammonia (NH3), nitrite and nitrate (NO2 + NO3), orthophosphate, salinity, chlorophyll a, and dissolved oxygen. In general, no significant spatial differences in these water quality parameter levels exist in the study area. The dissolved inorganic carbon data is presented since DIC is thought to be limiting the phytoplankton growth in some circumstances (Paerl, 1983). Figure 2 shows that the DIC levels increase over time, reaching a

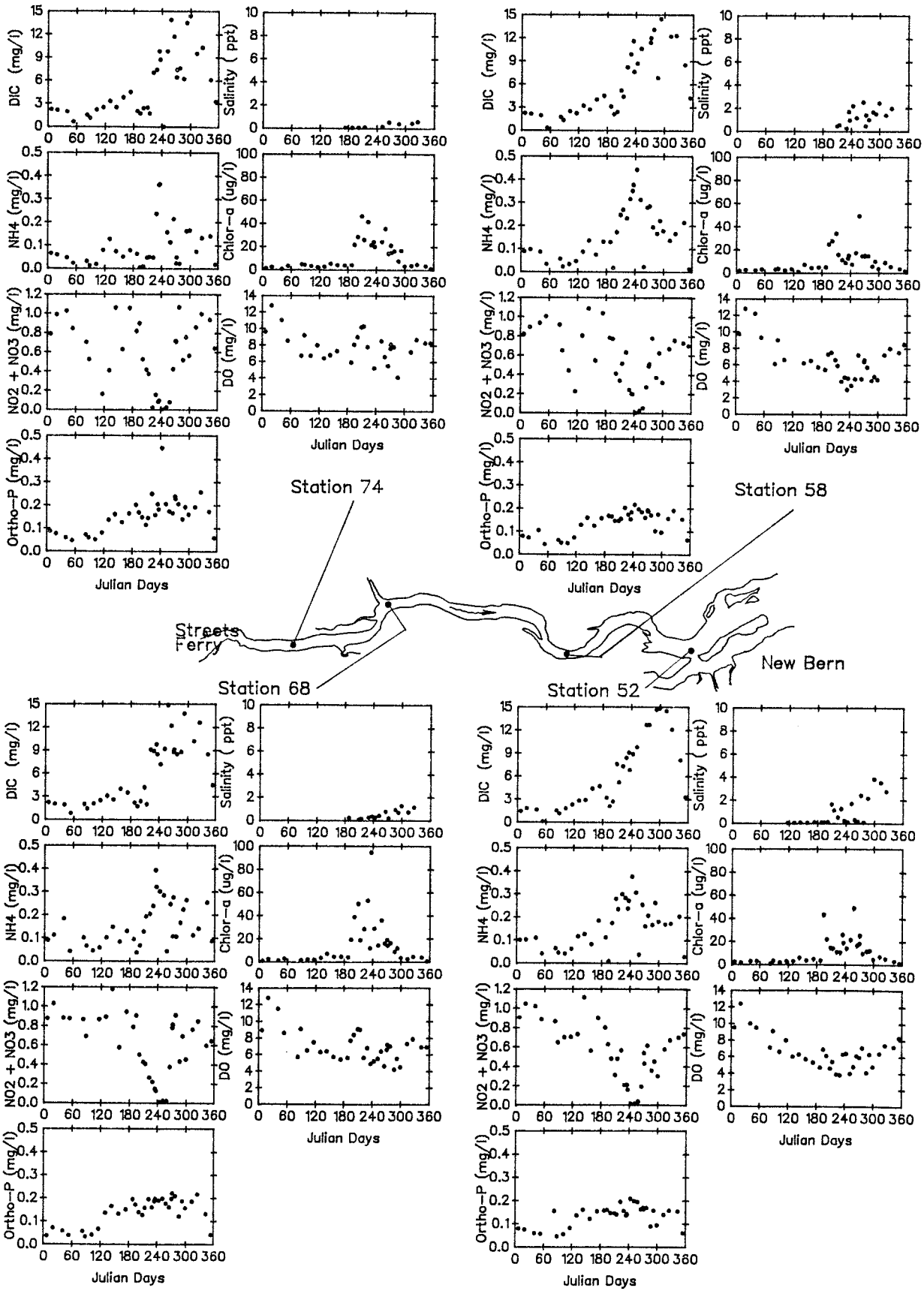

Figure 2. Observed Water Quality Conditions, 1983

maximum level of 15 mg/l before dropping down to 3 mg/l. The DIC levels are low in the first 3 months of the year. Ammonia follows a similar trend, reaching a maximum level about 0.4 mg/l on day 240. Nitrite and nitrate levels decrease to levels close to zero concentration before rising again. Nitrogen (NH_3, NO_2, and NO_3) are in sufficient supply in the water column for phytoplankton growth at the initiation of nuisance blooms. Similarly, orthophosphate concentrations are high in the lower Neuse River, thus would not be a limiting factor for phytoplankton growth at the initiation of nuisance blooms. The salinity level in the lower Neuse above the Streets Ferry bridge is generally low except during the summer low flow period when salinity intrusion reached this area. [The river flow at Kinston in 1983 is shown in Figure 3. The high spring runoff is followed by a relatively long period of low river flows in summer.] The chlorophyll a level of the phytoplankton biomass is low during the first 6 months of the year. Significant growth of phytoplankton associated with the blue-green bloom is observed in July, August, and September. Dissolved oxygen follows a decreasing trend in the first 6 months reaching minimum levels in July as the temperature in the water column increases progressively. A significant increase of the dissolved oxygen level near the surface follows the increase of chlorophyll a associated with the blue-green algae bloom (see Stations 74 and 68 in Figure 2). As the bloom disappears in October, the dissolved oxygen levels dropped before the increases again due to temperature decrease toward the end of the year.

A close examination of the ammonia and chlorophyll a data from the upstream stations to the downstream stations reveals that while chlorophyll a levels (during the bloom) decreases slightly in the downstream direction, ammonia concentrations increases accordingly in the down-

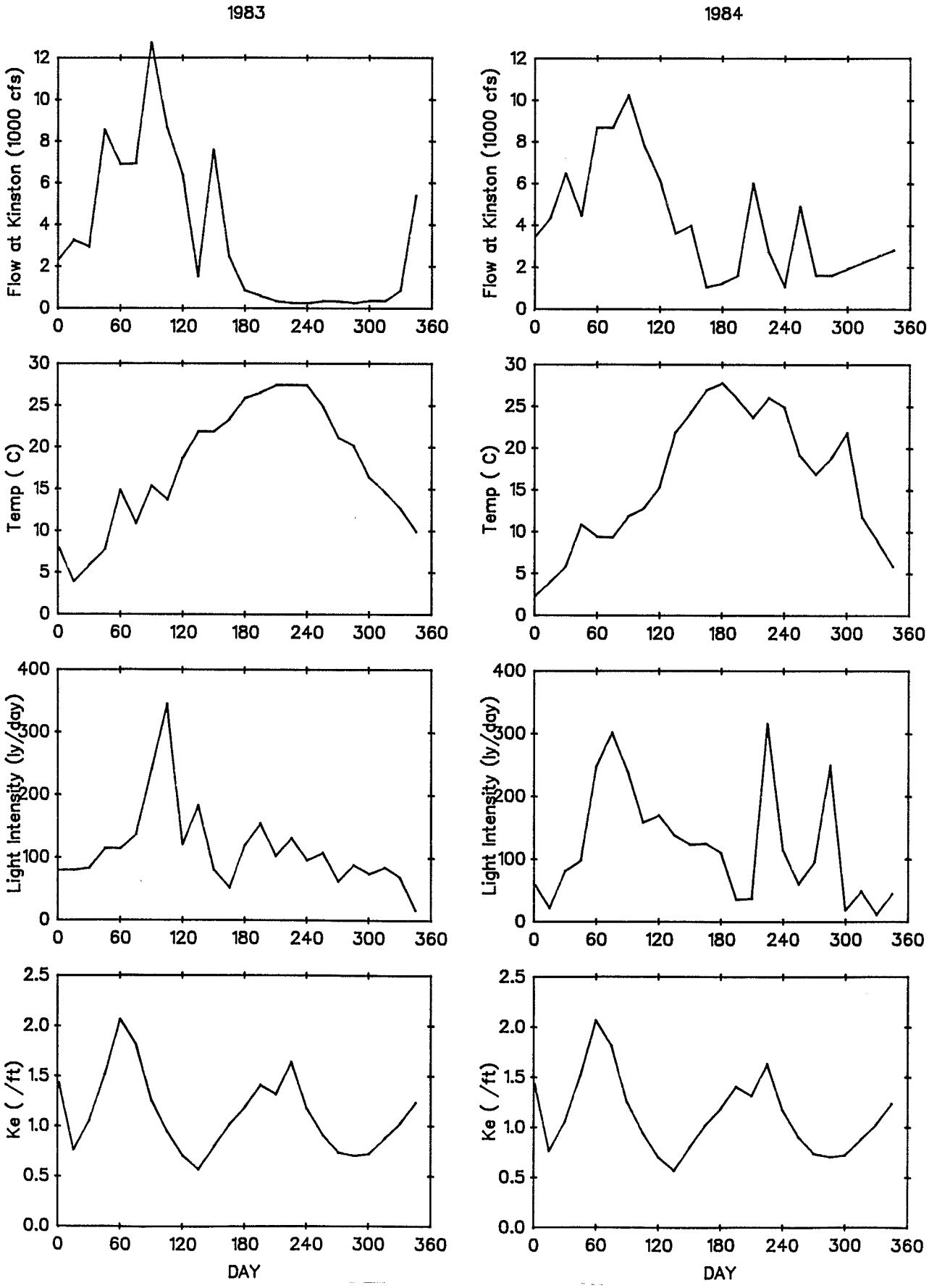

Figure 3. Flow, Temperature, Light Intensity, and Light Extinction Coef.

stream direction. Such an observation suggests nitrogen recycling from the phytoplankton biomass although some ammonia may come from the Weyerhauser plant.

In this study, phytoplankton species data was available from the Institute of Marine Sciences and reported in cells/ml. In order to obtain species chlorophyll a values, the cell count data was broken down into the four functional groups. For each cell count sample, the percentage of the total cells/ml was determined for each group. Those percentages were then used to determine the chlorophyll a for each species from the total chlorophyll a data. It should be stressed that different species of phytoplankton contain different amounts (per cell) of chlorophyll a. The approximation used in this study to derive the chlorophyll a concentrations for the four functional groups may therefore not generate accurate results. However, it is the most reasonable result that can be obtained given the available data (Mitchell, 1985). The derived chlorophyll a concentrations (in 1983) on a functional group basis are presented in Figure 4 for the same sampling stations where other water quality data was collected. The results show that during the bloom period non-nitrogen fixing blue-green algae is the dominating group in the phytoplankton biomass. The nitrogen fixing blue-greens are also present but at a much less pronounced level. Both diatoms and green algae are present at very modest levels during the bloom period.

2.3 Water Quality Data of 1984

The water quality data of 1984 is presented in Figure 5. One major difference between the 1983 data and the 1984 data is that the phytoplankton biomass level in 1984 is lower than the level in 1983. In fact, there was no blue-green algal bloom in the summer of 1984 while

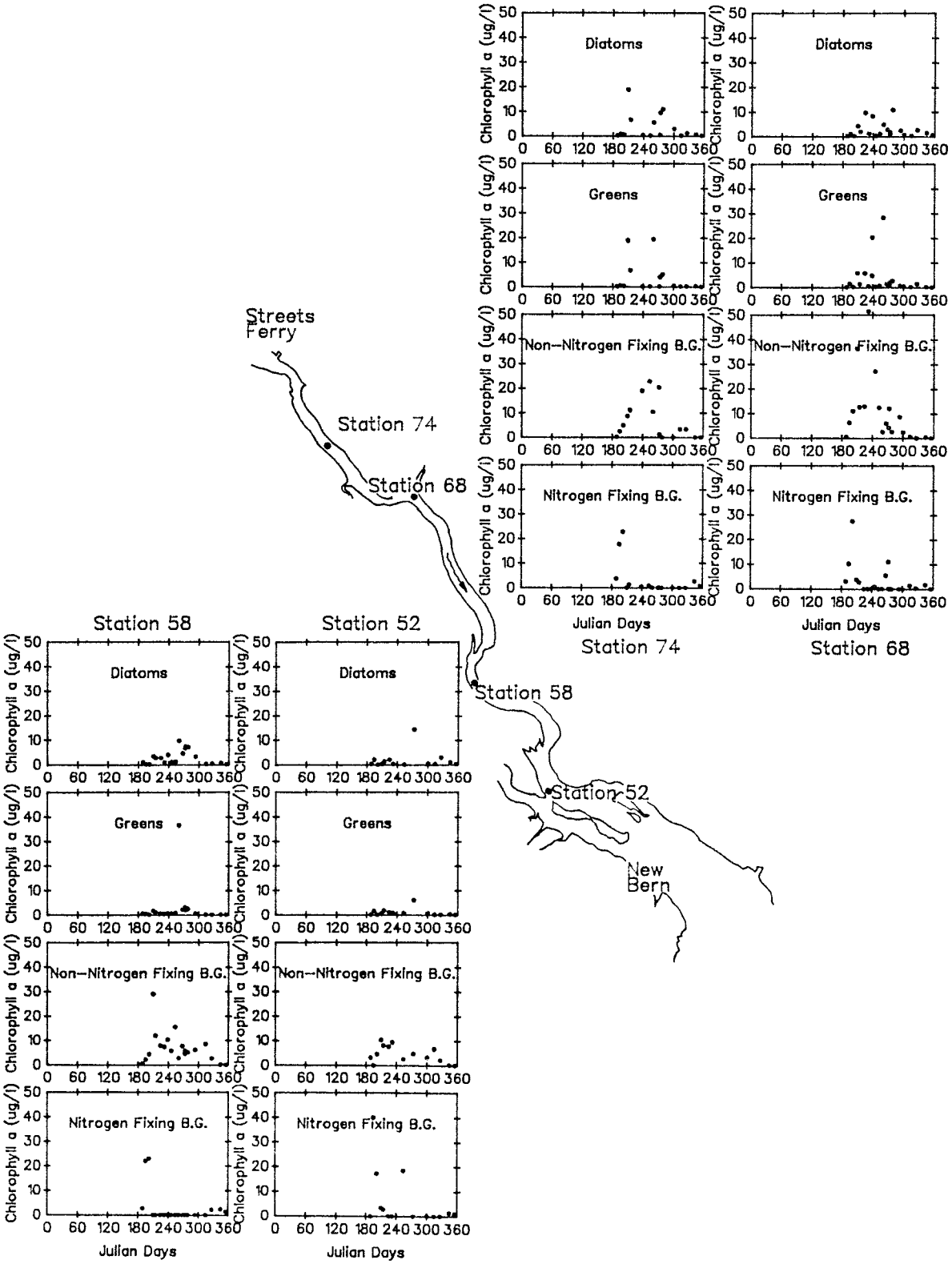

Figure 4. Algal Species Chlorophyll a Concentrations, 1983

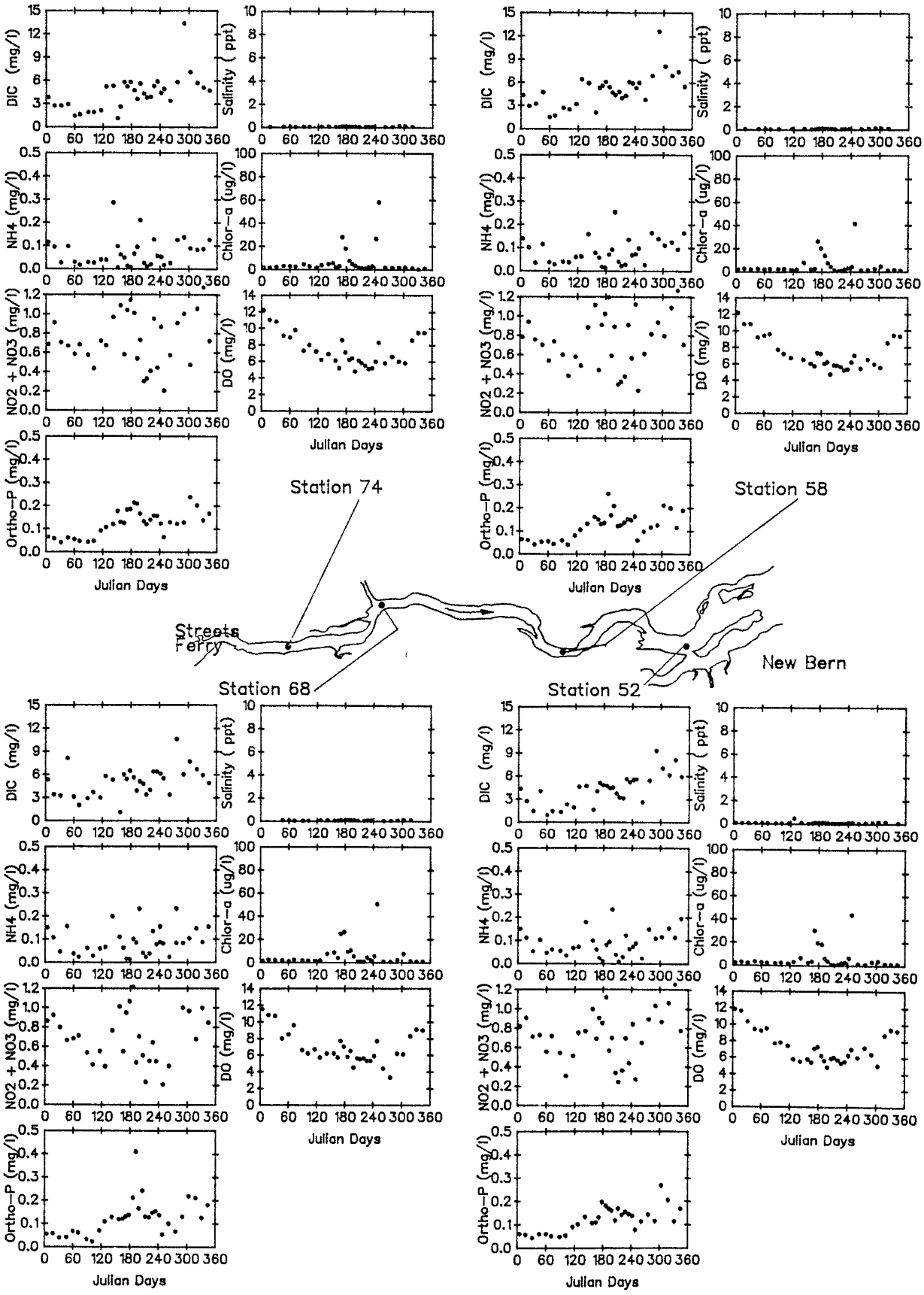

Figure 5. Observed Water Quality Conditions, 1984

the environmental conditions supported a modest growth of phytoplankton population. The disappearance of the blue-green algal bloom in 1984 is primarily due to flushing from the higher freshwater flow in the summer months (see Figure 3).

Because of the increased freshwater flow in the summer of 1984, salinity intrusion did not reach the study area (see Figure 5 for Station 52). The nutrient (NH_3, NO_2+NO_3, and orthophosphate) concentrations in 1984 were close to those observed in 1983 and appeared in sufficient supply to support the phytoplankton growth.

The algal species chlorophyll a data of 1984 is presented in Figure 6. Although there was no pronounced algal (surface) bloom in 1984, the non-nitrogen fixing blue-greens were still the dominating species (in terms of chlorophyll a level) throughout the year.

2.4 Factors Affecting Blue-Green Algal Blooms in the Lower Neuse River

Following the examination of the 1983 and 1984 data, the physical, chemical, and biotic factors suspected of playing a role in the establishment and proliferation of blue-green algal (Microcystis aeruginosa) blooms in the lower Neuse River are: (1) excessive (for algal growth) concentrations of both nitrogen and phosphorus nutrients throughout much of the year [at least at the initiation of blooms (period from May to July) nutrient levels appear to be sufficient for the maintenance of growth], (2) periods of low flow and decreased turbulence (vertical mixing), leading to thermal stratification of the water column. Periods of thermal stratification, even lasting only a day or two, are instrumental in promoting dominance by surface-dwelling Microcystis populations, thereby increasing overall bloom potential and resulting water quality degradation (Paerl, 1983). A combination of these physical and chemical agents leads to maximal bloom development. This was directly

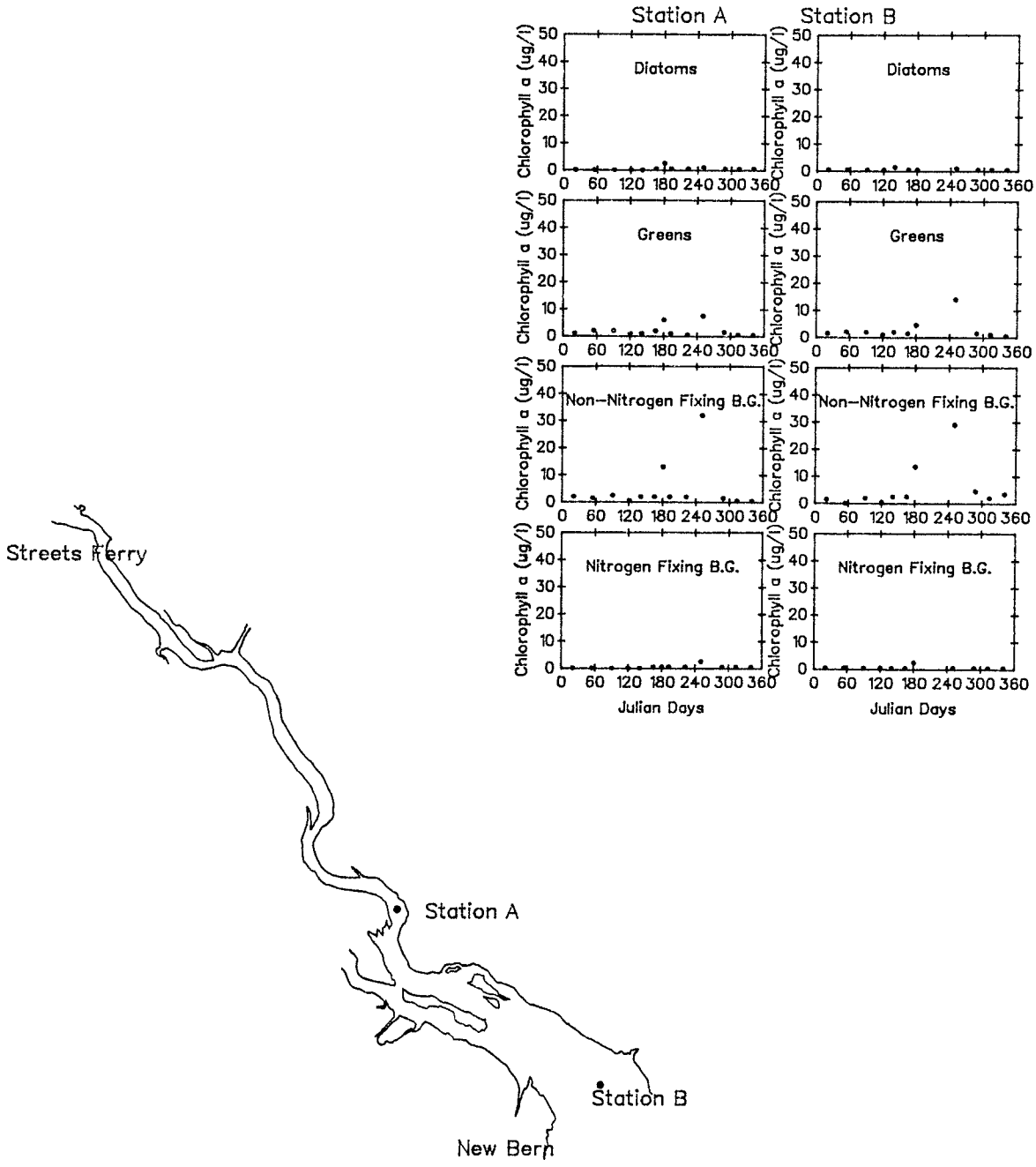

Figure 6. Algal Species Chlorophyll a Concentrations, 1984

observed in the summer of 1983 when dry, warm and calm weather, combined with excess nitrogen (mainly as NO_3) and phosphorus (as PO_4) concentrations led to several bloom periods in the summer months. In contrast, 1984, which witnessed abundant rainfall in spring and summer months, resulted in high river-flow velocities. Despite accompanying excess nitrogen and phosphorus loading, bloom development was not observed in 1984. The consistently high flow periods severely hampered the ability of Microcystis to become a nuisance bloom organism during 1984.

The same theory was also found valid with the 1981 and 1982 conditions. That is, there were blue-green algal blooms in the summer months of 1981 due to day, warm and calm conditions while no significant blue-green blooms were observed in 1982 when the river flows were high in summer (Paerl, 1983). Such a theory for the establishment and maintenance of blue-green blooms in the lower Neuse may be summarized in Table 1 to provide a better perspective.

The model developed in this study is designed to incorporate the factors in Table 1 on a quantitative basis. That is, the developed model is used to test the above described hypothesis of blue-green algal blooms in the lower Neuse River.

2.5 Use of Field Data

The field data from the lower Neuse River have supported and aided the modeling activity in several ways. In the first place, they have been used in aiding model construction through the quantification of coefficients in the model. For example, light measurements have been used to determine the light extinction coefficient in the water. The second use of the data has been to provide imput to the model, specifically in terms of system loadings, boundary conditions, and initial conditions for model computations. For example, upstream nutrient

loading rates have been estimated using the flows and concentrations at the model upstream boundary. Finally, the field data have also been utilized to verify the model. Each of the uses will be presented and discussed in detail in later sections.

Table 1. Factors Affecting the Bloom Potential

Factor	Effect
River Flow	Sustained (more than several weeks) summer low flow periods provide favorable conditions for the bloom
Temperature	Long warm summer months (June-October) favor the blue-green algal blooms
Hydrodynamics	Affecting mixing, salinity intrusion, stratification and mass transport, and success of nuisance surface bloom persistence
Salinity Intrusion	Secondary impact on algal bloom by negatively affecting the growth rate of some nuisance blue-green algae (including Microcystis)
Turbidity	Limit the growth of diatom and green (non-surface growing algae) in the deeper water and the growth of the near surface non-buoyant blue-greens
Carbon	Dissolved inorganic carbon levels are relatively low compared with phosphorus and nitrogen in terms of requirement for algal growth
Phosphorus	Consistently high phosphorus (particularly ortho-phosphorus) levels provide more than sufficient phosphorus for algal growth and bloom
Nitrogen	High ammonia and nitrate levels exist. What is especially crucial is the fact that nitrate sufficiency is common during the initial stages of bloom formulation (May-July).

3. MODEL DEVELOPMENT

3.1 Estuarine Eutrophication Models

There are a number of estuarine eutrophication models which have been reported in the literature (Thomann and Fitzpatrick, 1982; HydroQual, 1981; Di Toro et al., 1971; Thomann et al., 1974). The Potomac Estuary Model (PEM) was completed by HydroQual in 1982 to simulate the complex interactions that led to the advanced state of eutrophication found in the Potomac Estuary (Thomann and Fitzpatrick, 1982). PEM incorporates a state-of-the-art understanding of the kinetic processes involved in phytoplankton growth and death. In addition, studies of the Potomac Estuary show that interactions between the water column and the sediment could be important to the eutrophication process. For that reason, PEM also includes sediment mechanisms such as nutrient release and sediment oxygen demand. It is an extensive model involving eleven system variables: phytoplankton carbon, dissolved organic phosphorus, particulate organic phosphorus, dissovled inorganic phosphorus, particulate inorganic phosphorus, total organic nitrogen, ammonia, nitrate-nitrite, chlorides, carbonaceous biochemical oxygen demand, and dissolved oxygen. The Potomac Estuary is divided into seventy-six segments which include thirty-eight water column segments and thirty-eight sediment layer segments.

A water quality model for the Patuxent River Estuary has been developed by HydroQual (1981). It includes fourty-seven segments and nine system variables: chlorophyll-a, organic nitrogen, ammonia, nitrite, nitrate, organic phosphorus, orthophosphate, carbonaceous BOD, and dissolved oxygen. The water column was sliced into two layers in order to incorporate the proper mass transport pattern found in the

Patuxent Estuary. On a tidally averaged basis, the circulation consists of a horizontal seaward velocity in the upper layer and a landward velocity in the lower layer. A vertical velocity is introduced by this pattern in order to maintain hydraulic continuity.

3.2 Conservation of Mass

The framework of analysis detailed in this report is based upon the principle of conservation of mass. Simply stated the conservation of mass accounts for all of a material entering or leaving a body of water, transport of material within the water body, and physical, chemcial, and biological transformations of the material. The theoretical treatment of conservation of mass is presented in the Appendix. The modeling framework employed in this study, then, is made up of three components--the transport, due to freshwater flow and dispersion, the kinetic interaction between variables, and the external inputs.

3.3 Time and Space Scales

One of the principal decisions to be made in the choice of a modeling framework is the determination of the appropriate time and space scales. A problem context may involve several levels of time and space scales, such as variations in dissolved oxygen from hour to hour or month to month. There are two aspects to the time and space scale determination: (a) the temporal and spatial extent of the water quality problem and variable, and (b) the temporal and spatial interval of the computation, i.e., the time step and spatial grid dimensions of the computational scheme.

In a recent modeling study of the Potomac Estuary, Thomann and Fitzpatrick (1982) discussed various time and space scales associated with different water quality problems in an estuarine environment. The

Neuse River Estuary, in many aspects, resembles the Potomac River Estuary. The recent data of the Neuse River, as presented in Section 2, have indicated significant freshwater phytoplankton (blue-green algae) blooms occurring in the study area, with varying degrees of spatial extent. Furthermore, blue-green algal taxa in both systems are dominated by non-nitrogen fixing genera, including Microcystis and Oscillatoria. Generally algal growth begins in late spring, attains peak chlorophyll a levels during the summer and is marked by declining populations in the fall, although some short lived blooms have been observed during late fall and early winter. To address these facts and the issues of possible nutrient control strategies and resultant algal biomass, an intermediate spatial scale (10-20 miles) is appropriate while a seasonal or month to month time scale is required. An intermediate spatial scale dictates model segment sizes that are in the order of one to three miles in length, and would require modeling only 10 miles of the lower Neuse River. A seasonal or month to month time scale could be satisfied with an integration time step on the order of a day. A finer time scale, for example, minute to minute or hour to hour is not appropriate for algal growth dynamics, since all of the inputs that are relevant to the growth dynamics cannot be specified on so fine a time scale, and especially since phytoplankton population does not significantly vary from hour to hour. Computationally, however, the integration time step may be required to be less than a day in order to meet the stability criteria dictated by the numerical methods used to solve the mass balance equations (to be discussed later in Section 3.8, Computational Framework).

3.4 Model Segmentation

The study area is divided into twelve longitdinal segments beginning at Ft. Barnwell and ending about 3.3 miles upstream from New Bern (Figure 7). Blue-green algal blooms have been observed in this area during the past decade. The notorious scum forming genus, Microcystis, is particuarly dominant during summer stratification, when low ambient inorganic carbon levels and suboptimal subsurface light levels induce buoyancy and hence a surface existence (Paerl and Ustach, 1982; Booker and Walsby, 1982). The water column in the river from Streets Ferry and New Bern (6 segments) is therefore sliced into two layers. Thus, a total of 18 segments are used in the model (Figure 7). The geometry of the segments is presented in Table 2.

The two-layer segmentation is designed to better represent the physical system for two major reasons. It characterizes the salinity intrusion and mass transport in partially mixed estuaries such as the lower Neuse River. More importantly, this feature of the model takes into account the different growth kinetics associated with various functional groups of algae and the tendency for the blue-greens to congregate near the water surface. Gathering at the surface is an important factor in the blue-green's ability to outcompete other (eukaryotic) algal genera during blooms (Paerl, 1986).

3.5 Model Variables

An important criterion for the inclusion of variables in the calculation is the existence of adequate field data for the variable, as well as its importance in the processes being considered (Thomann and Fitzpatrick, 1982). Due to data constraints, it was decided to include the minimum number of state variable possible and yet to mimic the growth dynamics associated with multiple functional groups of algal

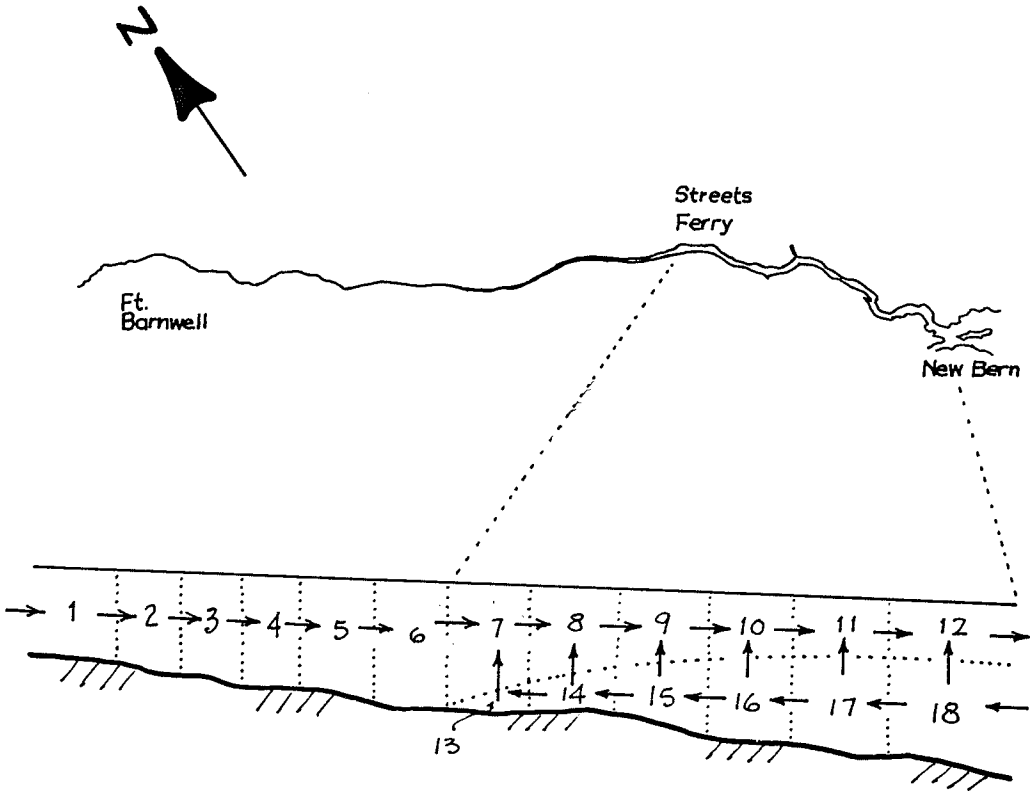

Figure 7. Model Segmentation

Table 2. Model Segment Geometry

Segment Number	Mean Depth (ft)	Volume (10^6 ft^3)
One Layer		
1	9.30	47.10
2	10.00	48.58
3	10.50	48.79
4	11.10	45.83
5	11.70	42.24
6	12.40	47.10
Surface Layer		
7	7.62	21.93
8	7.44	20.82
9	8.46	24.12
10	8.04	23.56
11	8.64	23.49
12	5.58	11.73
Bottom Layer		
13	5.08	14.62
14	4.96	13.88
15	5.64	16.08
16	5.36	15.71
17	5.76	15.66
18	3.72	7.82

species. As a result, the following eleven state variables were incorporated in the Neuse Estuary Eutrophication Model framework:

(1) Diatom chlorophyll a
(2) Green algal chlorophyll a
(3) Non-nitrogen fixing blue-green algal chlorophyll a
(4) Nitrogen fixing blue-green algal chlorophyll a
(5) Organic nitrogen
(6) Ammonia nitrogen
(7) Nitrite and nitrate nitrogen
(8) Organic phosphorus
(9) Orthophosphate
(10) Salinity
(11) Dissolved oxygen

Although nutrient levels are not limiting the algal growth (except during a low nitrate period in the 1983 bloom) in the lower Neuse, nutrient components are included in the model kinetics for assessing the impact of future nutrient control. It is known that zooplankton grazing of algae (particularly the diatoms and greens) is part of the nutrient recycle process in the water column. However, the zooplankton biomass is insignificant in the bloom area and as a result, not considered as a state variable. That is, nutrient recycling through zooplankton grazing is not important in the lower Neuse (Paerl, 1983). Other variables, constructed from these primary variables are also tracked through the lower Neuse River. These secondary variables include total phytoplankton chlorophyll a, total nitrogen and total phosphorus as the most important.

The kinetic equations discussed below that incorporate the above state variables are designed to simulate the annaul cycle of phytoplankton production, its relation to the supply of nutrients, and its potential effect on dissolved oxygen. The calculation is based upon formulating the kinetics which govern the interactions of the biota and the forms of the nutrients and applying them to the regions of the lower Neuse River within the context of conservation of mass equations.

3.6 Mass Transport

The two components of transport, advective flow and dispersion, are responsible for the movement of the water quality constituents within the estuary. The advective flow transports the water quality constituents from the upstream freshwater or riverine portion of the estuary to the downstream, tidally dominated, salinity portion of the estuary and accounts for the instream dilution of point and nonpoint wastewater discharges. Another advective flow which transports salinity from the estuarine portion to the riverine portion in an upstream direction is usually observed in the lower Neuse River (Giese et al., 1985). This is a typical estuarine circulation pattern where more saline bottom water ("wedge') enters the estuary and moves in the upsteam landward direction. This flow is balanced by a downstream flow of less saline water in the upper layer. There is a continual transport (vertical advective flow) and exchange of water (vertical mixing) between the lower and the upper layers.

A simple and efficient method of analysis of this type of mass transport has been developed (O'Connor and Lung, 1981; Lung and O'Connor, 1984). The analysis is based on the condition that the salinity distribution in both the longitudinal and vertical planes are known or may be assigned. The advective and dispersive transport mechanisms associated with the given salinity distribution can be quantified and can then be incorporated into the mass transport equation of salinity. Solutions of the mass transport equation yield the salinity distributions, which may then be compared with the given or known salinity distribution to verify the mass transport.

3.7 Kinetics Formulations

Figure 8 presents the principal kinetic interactions for the nutrient cycles, dissolved oxygen, and four algal functional groups. Orthophosphate is utilized by algae for growth. Phosphorus is returned from the phytoplankton biomass pool to organic phosphorus and to orthophosphate through re-excretion and non-predatory mortality. Organic phosphorus is converted to orthophosphate via micro-mineralization and hydrolysis at a temperature dependent rate.

The kinetics of the nitrogen species are fundamentally the same as the phosphorus system. Ammonia and nitrate are used by phytoplankton for growth. The rate at which each is taken up is proportional to its concentration relative to the total inorganic nitrogen (ammonia plus nitrate) available. Nitrogen is returned from the algal biomass and follows pathways that are similar to phosphorus. Organic nitrogen is converted to ammonia via hydrolysis and mineralization at a temperature dependent rate, and ammonia is then converted to nitrate (nitrification) at a temperature dependent rate.

Dissolved oxygen is coupled to the other system variables. The sources of oxygen considered are reaeration and evolution by phytoplankton photosynthetic production during growth. The sinks of dissolved oxygen are algal respiration, oxidation of detrital carbon, nitrogen and phosphorus and carbonaceous material from waste effluents and nonpoint discharges, sediment oxygen demands, and nitrification, if any.

Algal growth and death kinetics are formulated for each algal group on an individual basis. Algal growth rates vary from one group to another. For nitrogen fixing blue-greens, no nitrogen limitation is

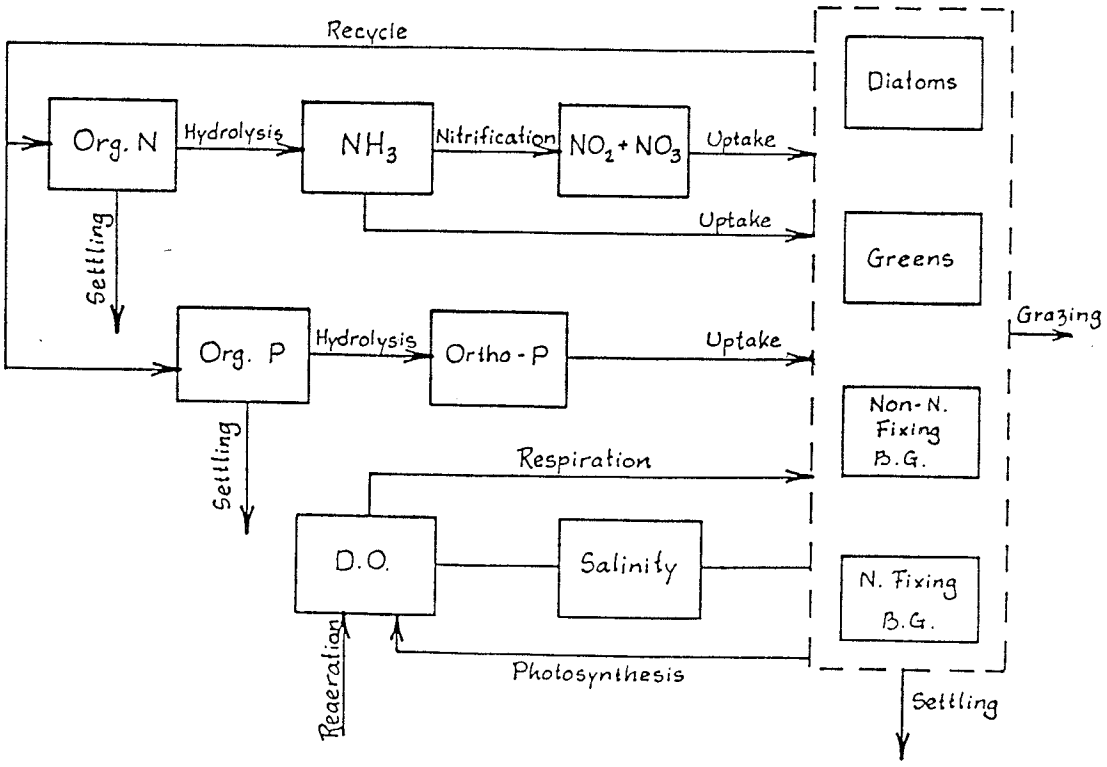

Figure 8. Neuse Estuary Eutrophication Model Kinetics

incorporated. In addition to light and nutrient limitations, salinity effect on the algal growth is also included. Specific details for the above reactions are presented below.

Phytoplankton Kinetics

Although the model handles four functional groups separately, the basic growth rate formulation is the same for each functional group. The growth rate of phytoplankton is a function of temperature, light, nutrient concentration and salinity level. The growth coefficient is directly related to temperature in moderate climates. Auer and Canale (1980) and Canale and Vogel (1974) summarized data from phytoplankton growth experiments conducted at various temperatures. These results, plotted as the solid and dashed lines in Figure 9, illustrate the different temperature optimums for different phyla of phytoplankton and also the differences in the way temperature influences growth rate. Essentially, Figure 9 is incorporated into the Neuse Estuary Eutrophication Model to characterize the growth rates as a function of temperature for diatom, green, and blue-green species. Figure 9 shows that at temperatures below 30°C, diatoms have the highest growth rate and the blue-greens have the lowest growth rate.

The growth rate of phytoplankton is also dependent on the light intensity up to a saturating condition, greater than which it may decrease with light. The growth rate at saturating light condition can be expected to be species dependent as shown in Figure 10. Because light energy available to phytoplankton varies so much with depth and time of day, an appropriate expression of light availability for use in analyses should account for these changes. A depth and time averaged effect of available light energy on phytoplankton growth rate can be

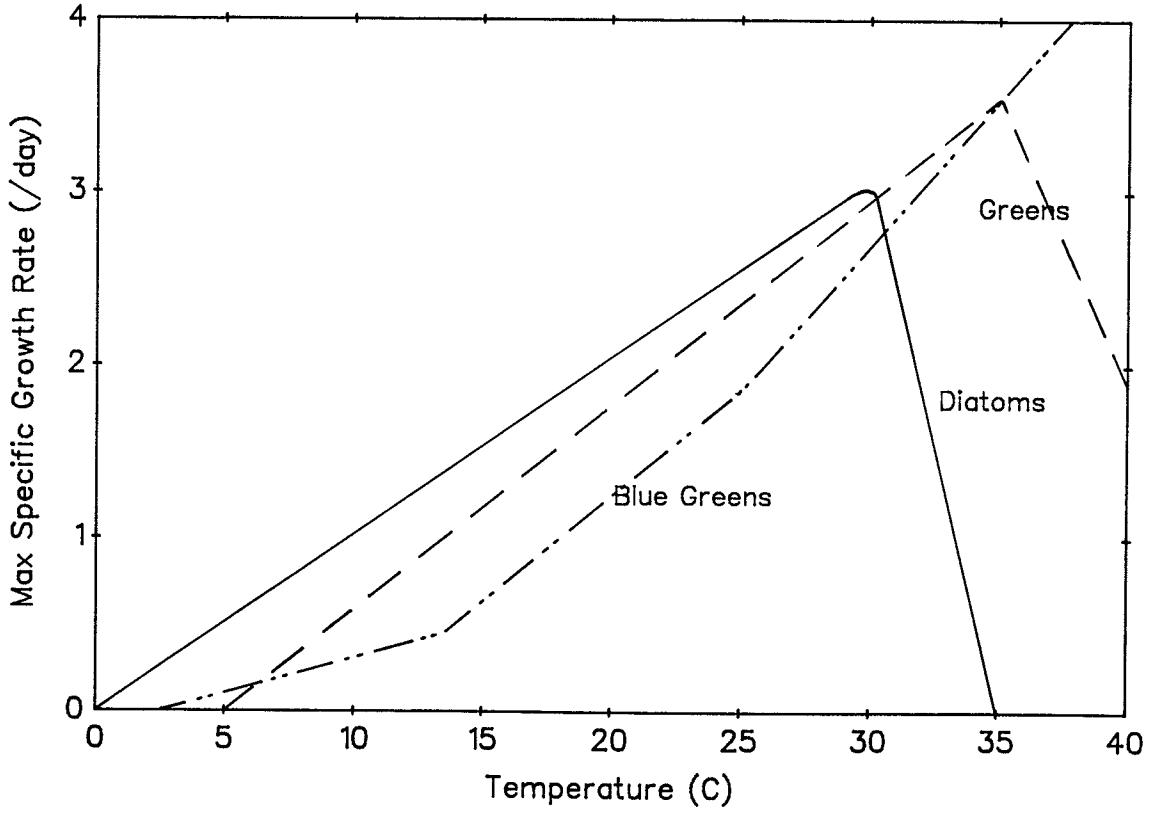

Figure 9. Specific Growth Rate as Function of Temperature

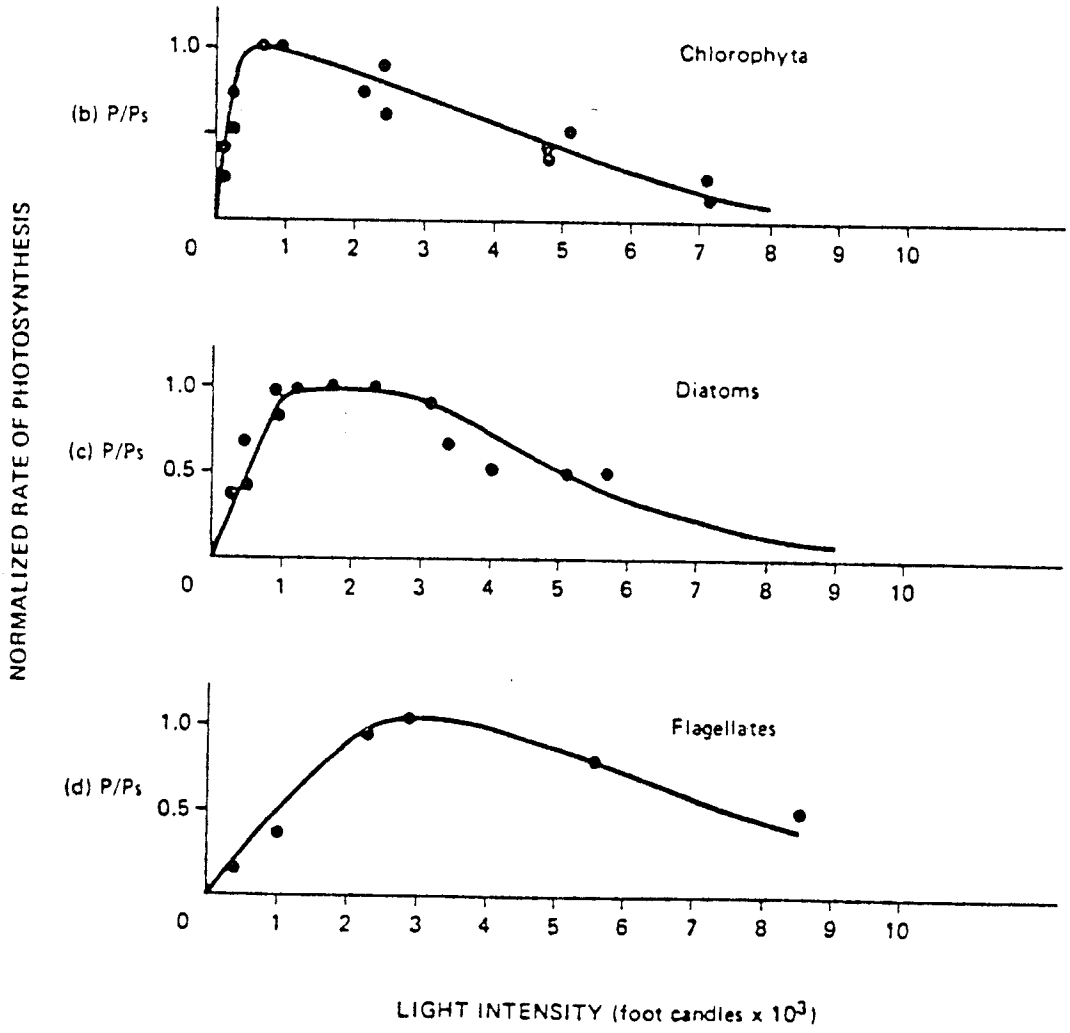

Figure 10. Effect of Light Instensity on Algal Growth

obtained for the Neuse River Estuary, by integrating the light intensities relationships over depth and time. This reduces to

$$r_L = \frac{2.718f}{K_e HT}\left(e^{-\frac{I_f}{I_s}e^{-K_eH}} - e^{-\frac{I_f}{I_s}}\right) \quad (1)$$

where r_L = light limitation factor
f = photoperiod - daylight fraction of averaging period
T = averaging period (1.0 day)
K_e = light extinction coefficient (1/ft)
H = average depth of segments (ft)
I_a = average of incident light on water surface over 24 hour day
I_f = average of incident light over photoperiod (= I_a/f)
I_s = saturated light intensity

Similarly, the growth rate is also a function of nutrient concentrations up to a saturating condition, greater than which it remains constant with nutrient consentration. Such a relationship is described by a Michaelis-Menton formulation whose significant parameter is that concentration at which the growth rate is equal to one-half of that at the saturated concentration. When both nitrogen and phosphorus are involved, the growth rate is assumed to be proportional to the product of the Michaelis expressions for each of the nutrients. In the lower Neuse River, silica is not considered a limiting nutrient for diatoms and therefore is not included in the model. Thus, the nutrient reduction factor, r_N, is of the form

$$r_N = \frac{N}{K_N+N}$$

where N = the nutrient concentration (µg/l)
K_n = half saturation (Michaelis) constant (µg/l)

The Michaelis constant is a function of algal species. Their values usually range from 5 µg/l to 25 µg/l for nitrogen and from 1 µg/l to 5

µg/l for phosphorus, depending on the species. In NEEM, different Michaelis constant values are allowed for different phytoplankton functional groups.

There is a general consensus that most freshwater algal species exhibit a decrease in biomass in low salinity waters (Paerl et al., 1984; Morris et al., 1982; Sharp et al., 1982; Pennock, 1983). The salinity effect in the model is incorporated using specific algal thresholds for salinity. The salinity thresholds (in parts per thousand, ppt) describe that particular algal species' tolerance to saline conditions. Currently, this is considered an empirical approach to quantifying the effect that salinity has on the growth rate of freshwater algae (see Figure 11). The growth rate is not affected by salinity until the salinity level reaches the first threshold, S_1 (i.e., the salinity reduction factor is 1.0). The salinity reduction factor decreases linearly between log S_1 and log S_2. When the salinity reaches the second threshold, S_2, the salinity reduction factor is at its minimum (i.e., the salinity effect is greatest). The values of 1 ppt and 2 ppt are used in the model as S_1 and S_2, respectively, while the minimum salinity reduction factor is set at 0.4. These values are based on observations that show a narrow range of tolerance that freshwater algal species have for salinity (Filardo, 1984).

The phytoplankton growth rate can be formulated as follows:

$$G_p = K_T(T)\,\frac{2.718f}{K_e HT}\left[e^{-\frac{I_f}{I_s}e^{-K_e H}} - e^{-\frac{I_f}{I_s}}\right]\frac{Ni}{K_{MN}+Ni}\cdot\frac{P}{K_{Mp}+P}\cdot r_s \qquad (2)$$

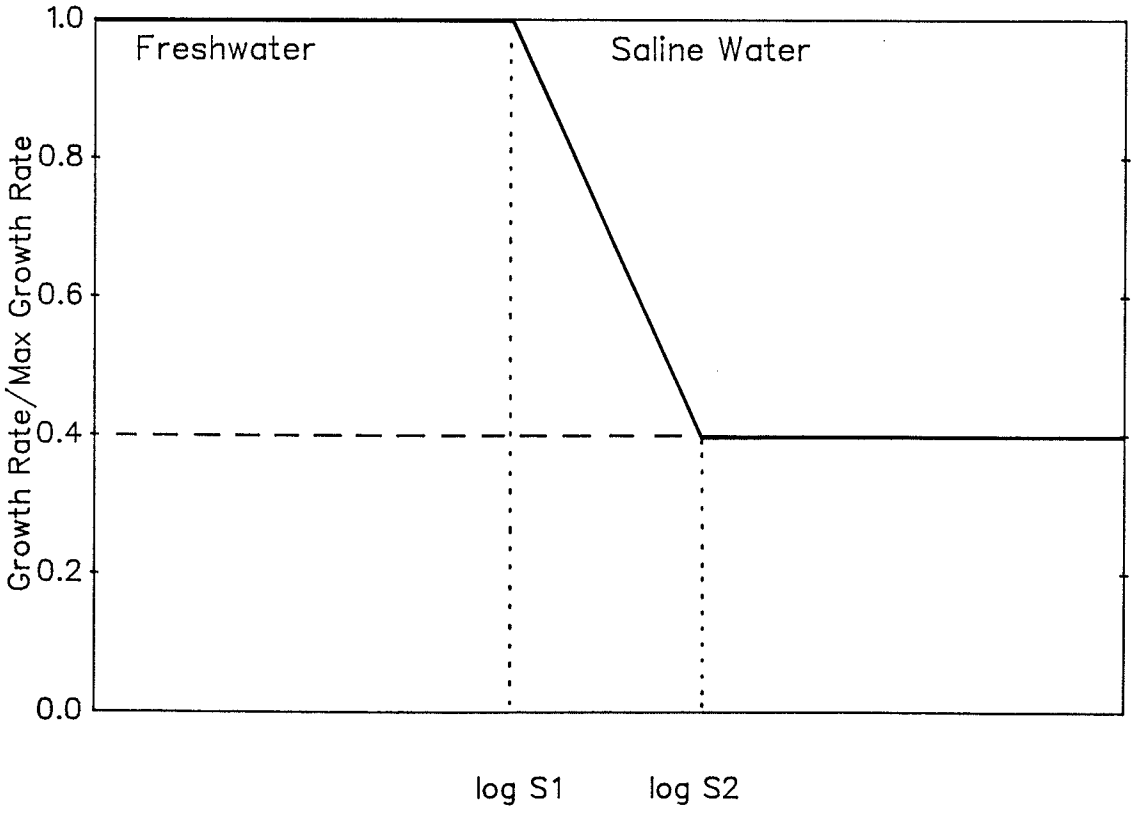

Figure 11. Salinity Effect on Algal Growth Rate

where $K_T(T)$ = temperature dependent growth rate (see Figure 9)

Ni = inorganic nitrogen concentration (sum of ammonia, nitrite, and nitrate)

P = Ortho-phosphorus concentration

r_s = salinity reduction factor (see Figure 11)

Decreases in algal biomass concentrations are brought about by three processes:

(a) endogenous respiration

(b) death and grazing

(c) algal settling

Algal respiration is caused by endogenous respiration. Algal death includes grazing by zooplankton (for diatoms and greens only) and cell destruction through bacterial attack, disease, physical damage, the natural aging process or other mechanisms. Grazing by zooplankton is primarily limited to diatoms and greens although some blue-greens may be grazed by crustacean zooplankton at reduced rates. In addition, protozoans and rotifers can consume blue-greens (including Microcystis). In the model, approximations are made that only the diatoms and greens are consumed by the zooplankton. The distinction between phytoplankton reductions through death and reductions through respiration, grazing by zooplankton, or settling is that upon death, all the carbon, nitrogen and phosphorus contained in the algal biomass is returned to the carbonaceous BOD and organic nitrogen and phosphorus pools, respectively. During respiration, carbon is given off as CO_2 rather than CBOD; through grazing, only 40% of the organic contents of the algal cells is returned to the respective organic pools (the remaining 60% is lost from the balance as zooplankton biomass); through setting, none of the organic cell material is returned to the organic pools.

Settling rates of algae are specified in units of feet per day, and are internally converted to 1/day units on a segment by segment basis, according to segment depth.

The algal reduction rate can be expressed as:

$$D_p = K_1(T) + Dr - \frac{V_s}{H} \quad (3)$$

where $K_1(T)$ = temperature dependent endogeneous respiration rate
Dr = death rate
V_s = settling velocity
H = average segment depth

Nitrogen

The major components of the nitrogen system are detrital organic nitrogen, ammonia nitrogen, and nitrate nitrogen. In natural waters there is a stepwise transformation from organic nitrogen to ammonia, nitrite and nitrate, yielding nutrients for phytoplankton growth. The kinetics of the transformations are temperature dependent.

The equation for the kinetic term of the organic nitrogen system is:

$$S_{org.N} = (N/Chl)\ (Dr)\ (Chl) - (K_{34})\ \theta^{T-20}\ C_{org.N} \quad (4)$$

where N/Chl = nitrogen to chlorophyll ratio
Dr = phytoplankton death rate and respiration rate
K_{34} = ammonification (decay of organic nitrogen to ammonia) rate
$C_{org.N}$ = concentration of organic nitorgen in the system

The first term in Equation 4 represents the organic nitrogen that is released through endogeneous respiration by phytoplankton and phytoplankton death following the incorporation of the organic nitrogen equivalent of grazed but not metabolized phytoplankton excreted by

zooplankton. Since the model incorporates four groups of phytoplankton, the kinetic term involving phytoplankton is calculated separately for each species to allow for possible differences in rates between algal groups. The second term in Equation 4 describes the sink of organic nitrogen due to ammonification.

The reaction equation for ammonia is:

$$S_{NH_3} = K_{34}\,\theta^{T-20}\,C_{org.N} - K_{4s}\theta^{T-20}C_{NH_3} - G_p \bullet Chl \bullet N/Chl \bullet PNH_3 \qquad (5)$$

where K_{45} = nitrification rate
G_p = phytoplankton growth rate
PNH_3 = preferenced by phytoplankton for ammonia

The source of ammonia in Equation 5 is due to ammonification. Nitrification, the sequential oxidation of ammonia to nitrate, is the sink described in the second term of the equation. The last term quantifies uptake of ammonia by phytoplankton. Although both inorganic forms of nitrogen, ammonia and nitrate, are available for use in cell growth by algae; for physiological reasons the preferred form is ammonia. The ammonia preference is calculated by Thomann and Fitzpatrick (1982) for the Potomac Estuary as follows:

$$PNH_3 = NH_3 \bullet \frac{NO_3}{(K_{mn}+NH_3)(K_{mn}+NH_3)} + NH_3 \bullet \frac{K_{mn}}{(NH_3+NO_3)(K_{mn}+NO_3)} \qquad (6)$$

where K_{mn} = Michaelis constant for nitrogen (5 to 25 µg/l). The behavior of Equation 6 is most sensitive at low values of ammonia or nitrate. As one can see, for a given concentration of ammonia, as the available nitrate increases above approximately the Michaelis limitation the preference for ammonia reaches a plateau. Also as the concentration

of available ammonia increases the plateau levels off at values closer to unity, i.e., total preference for ammonia.

Nitrate kinetics are similar to those described in the ammonia system. Nitrification is now the source, with phytoplankton utilization being the only sink.

$$S_{NO_3} = K_{45} \cdot C_{NH_3} - G_p \cdot Chl \cdot N/Chl \cdot (1-PNH_3) \quad (7)$$

Phosphorus

The phosphorus system is similar in some respects to that of nitrogen. Organic phosphorus is generated by the respiration and death of phytoplankton. Phosphorus in this form is then converted to the inorganic state, approximated by orthophosphate, where it is available to the algae. The kinetic formulation for organic phosphorus is:

$$S_{org.P} = P/Chl \cdot Dr \cdot Chl - K_{67}\ \theta^{T-,20} \cdot C_{org.P} \quad (8)$$

where P/Chl = phosphorus to chlorophyll ratio
K_{67} = mineralization rate

The kinetic equation for orthophosphate is:

$$S_{PO_4} = K_{67} \cdot \theta^{T-20} \cdot C_{org.p} - P/Chl \cdot Gp \cdot Chl \quad (9)$$

In Equation 9, mineralization is the source of orthophosphate while the only loss of orthophosphate to the system occurs due to phytoplankton uptake.

Dissolved Oxygen

The addition of oxygen to the system are caused by production by phytoplankton photosynthesis and reaeration. The losses of oxygen result from phytoplankton respiration, nitrification, and benthic oxygen demand. In addition, oxygen is lost to the atmosphere during oxygen saturated bloom periods. The kinetic formulation is:

$$S_{DO} = Gp \cdot Chl \cdot O_2/Chl + (C_s - C_{DO})\ K_a - K_1(T) \cdot \theta^{T-20} \cdot O_2/Chl \cdot Chl$$

$$- K_{45}\theta^{T-20}C_{NH} \cdot 4.57 - K_{BN}/H \qquad (10)$$

where C_s = saturation concentration of dissolved oxygen as a function of temperature and salinity

K_a = reaeration coefficient

K_{45} = nitrification rate

K_{BN} = benthic oxygen demand

Salinity

Salinity is treated as a conservative substance in the model. It affects the phytoplankton growth rate (Equation 2) and the saturation concentration of dissolved oxygen.

3.8 Computational Framework and Effort

Before getting into the tasks of model calibration and sensitivity analyses, it is well to clarify the definition and meaning of the term "mathematical model." There are two principal components to a mathematical model. One component is concerned with the specific water quality problem context--the particular water body (its geometry, flow, dispersion), and the specific identification of the water quality problem. Thus for the Neuse, interests center on the lower Neuse and

the upper estuary and the problem at hand is eutrophication. Specification of the relevant variables (e.g., algal species chlorophyll a, phosphorus) must be made and the kinetic linkages or interactions between the variables must be specified as presented in preceeding sections. These interactions make up a theoretical construct which incorporates the major features of the eutrophication problem in the lower Neuse River. Finally, in this first component, a numerical specification of input loads, system parameters and environmental variables must be made. Such specification for eutrophication, for example, includes numerical values for the phosphorus recycle rate, the nitrogen levels at which phytoplankton growth is inhibited and incoming solar radiation. At this point, a set of variables, interactions and numerical specifications within the context of the lower Neuse River has been developed in the form of a set of interactive equations in time and space. In order to calculate the levels of the system variables, a computational scheme or framework must be used. This represents the second major component.

Available computational schemes include simple manual, desk top calculations as well as various degrees of complexity of computer software. In many water quality models (programs) available in the public domain, the basic variables and interactions are specified and it is generally not easy to change the number of variables or more importantly the complexity of the interactions. Following a close examination of these programs, the Water Quality Analysis Simulation Program (WASP) first developed by Hydroscience, Inc. and later documented for U.S. EPA (Di Toro et al., 1980) was chosen.

WASP has proved itself to be a very versatile program, capable of studying time variable or steady state, one, two or three dimensional, linear or non-linear kinetic water quality problems. To date WASP has been employed in many modeling applications, that have included river, lake, estuarine and ocean environments and that have investigated dissolved oxygen, bacterial, eutrophication and toxic substance problem contexts. WASP permits the modeler to structure one, two, and three-dimensional models; allows the specification of time-variable exchange coefficients, advective flows, waste loads and water quality boundary.

The Neuse Estuary Eutrophication Model was run on a Compaq micro-computer system installed with an 8087 math co-processor. A one-year simulation run of the model takes 5.5 hours on the Compaq. To speed up the model testing, debugging, and calibration processes, the model was uploaded from the microcomputer to the University of Virginia's CDC Cyber mainframe system. The model results are then downloaded and processed using a Hewlett Packard 7470A personal computer plotter.

4. MODEL CALIBRATION AND SENSITIVITY ANALYSIS

4.1 Derivation of Model Input

Prior to running the model for calibration, a significant amount of model input (e.g., time variable boundary conditions, initial conditions, and kinetic coefficients) needs to be developed. This section describes the derivation of the model coefficients and parameters.

Mass Transport

An important feature of the model is the two-layer mass transport pattern often found in partially mixed estuaries which is dependent on the extent of salinity intrusion. In the summer of 1983, the freshwater flows in the lower Neuse River were relatively low (see the flow at Kinston in Figure 3) resulting in salinity intrusion into the study area. On the other hand, the summer of 1984 was observed with relatively higher flows and salinity intrusion did not reach the study area. The simplified methodology proposed by Lung and O'Connor (1984) and O'Connor and Lung (1981) was employed to develop the two-layer transport pattern for the summer of 1983 using the data on freshwater flows and salinity distribution from the lower Neuse River. That is, time-variable two-layer transport patterns were developed in a 15-day interval for input to the model. The derived mass transport patterns were eventually validated by reproducing the salinity distribution in the lower Neuse on a time-variable basis. Figure 12 shows one of such mass transport patterns for 1983. The freshwater flow is in the downestuary direction in the upper layer and the upestuary flow is in the bottom layer. The sum of the horizontal flows is equal to the net freshwater flow at any given location. Vertical flows (in the upward direction) are introduced to maintain the hydraulic balance (Figure 12).

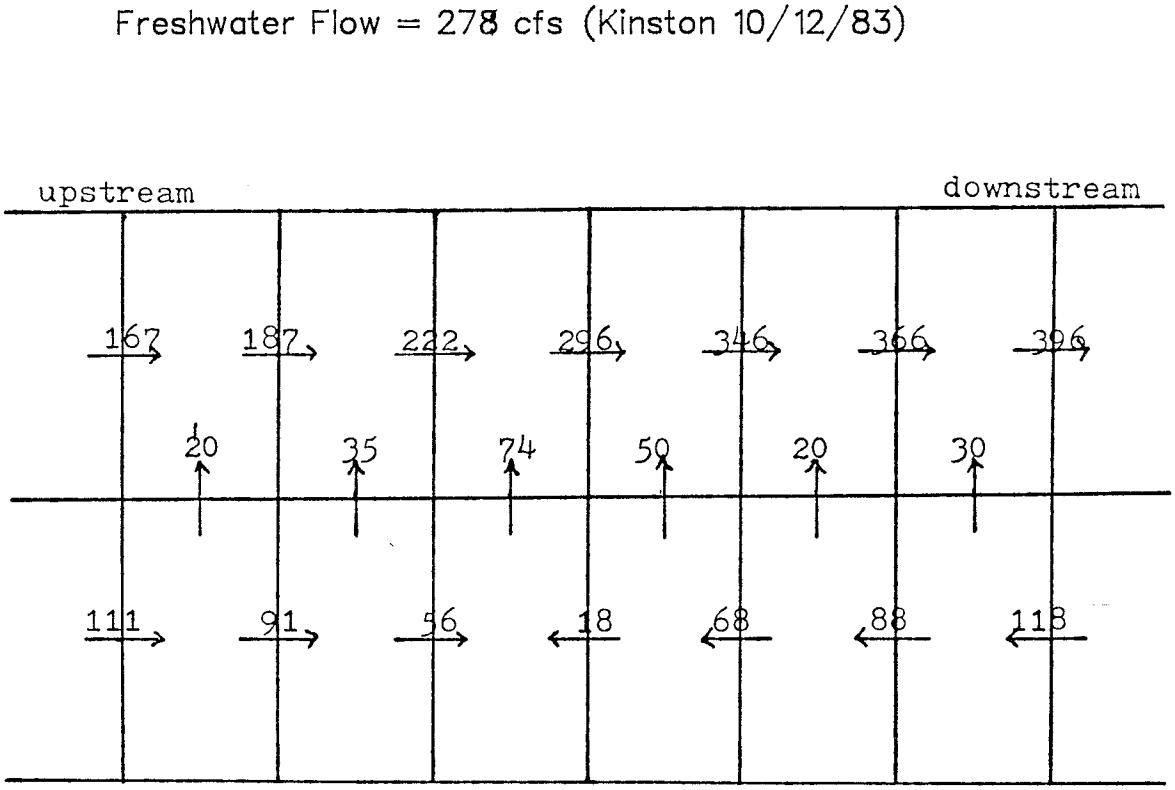

Figure 12. Two–Layer Mass Transport in the Lower Neuse River

Algal Growth Kinetics Coefficients and Parameters

The algal growth rates (/day) as a function of temperature are incorporated in the model as described in Section 3.7. The time-variable temperature input was derived from the temperature measurements in the field. Similarly, the surface light intensity (as photosynthetically available radiation, the light energy of wavelengths between 300 and 720 nm) was also from the field measurements. The photoperiod as a function of time over the year was obtained from the climatological data at Kinston. Table 3 shows the temperature, surface light intensity, and photoperiod data for 1983 as model input.

The penetration of light is limited by suspended materials such as clay and silt particles, by colored dissolved organic matter of humic nature and by the phytoplankton organisms. Measurements of light intensity at different depths in the water column were available. This information was summarized in terms of light extinction coefficients defined by the equation,

$$I/I_o = e^{-K_e z}$$

where z is the depth, I is the light intensity at depth z, I_o is the surface light intensity, and K_e is the light extinction coefficient. Estimates of K_e were obtained by fitting the above equation to data using a least-squares criterion for the plots of $\ln(I/I_o)$ vs z. The slope of the plot is the total light extinction coefficient. The light extinction due to algal self-shading is substracted from the total light extinction coefficient. The resulting value is input into the model which calculates the algal self-shading effect, particularly the surface-gathering blue-greens during the bloom period and adds to the light

Table 3. Temperature, Light Intensity, and Photoperiod (1983)

Day	Temperature (°C) Top Layer	Bottom Layer	Surface Light Intensity (Ly/day)	Photoperiod
1	8.0	8.0	81.0	0.473
15	4.0	4.0	81.0	0.479
30	6.0	6.0	84.6	0.484
45	8.0	7.8	115.8	0.528
60	15.0	15.0	115.8	0.572
75	11.0	11.0	138.9	0.611
90	15.5	15.5	243.1	0.649
105	14.0	13.6	347.3	0.655
120	19.0	18.5	122.7	0.660
135	22.0	21.9	185.2	0.671
150	22.0	22.0	81.6	0.682
165	22.0	25.0	53.2	0.671
180	25.0	27.0	121.6	0.660
195	27.0	26.4	156.3	0.644
210	27.0	28.2	104.2	0.627
225	29.0	26.2	133.1	0.600
240	27.0	28.0	97.3	0.572
255	29.0	21.0	109.9	0.523
270	21.0	21.5	63.7	0.473
285	22.0	18.5	90.3	0.457
300	18.0	15.0	75.3	0.440
315	16.0	13.5	86.8	0.440
330	14.0	11.5	69.5	0.429
345	12.0	8.0	17.4	0.418
360	5.0	2.5	60.2	0.446

extinction due to suspended particles. The time-variable light extinction coefficient (less self-shading effect) is shown in Figure 3. As described in Section 3.7, the total light extinction for the diatoms and greens also includes the shading from the blue-greens because the blue-greens usually stay near the water surface.

Other growth related coefficients and parameters were derived from laboratory and field empirical estimates as published in the scientific literature. Table 4 summarizes these values from a number of estuarine systems as well as the lower Neuse River.

Nutrients

The nutrient kinetic coefficients used in the Neuse River model are shown in Table 5 along with the representative values from the literature. It is seen that the values used in this study are within acceptable limits.

Dissolved Oxygen

The reaeration coefficient has been estimated by Equation 11 as a function of depth, tidal velocity, and wind speed:

$$K_a(\text{at } 20°C) = \frac{12.9\ U^{0.5}}{H^{1.5}} + 0.4\ \frac{W}{H} \qquad (11)$$

where U = average tidal velocity (ft/sec)
W = wind speed (mile/hr)
H = average segment depth (ft)

There was no wind speed data available for the study area. Thus, the windspeed was approximated using the data from the Potomac Estuary. Such an approximation is not expected to introduce serious errors in the model calculation as the wind-induced reaeration is usually not significant compared with the reaeration due to tidal currents. In

Table 4. Phytoplankton Kinetics Parameters and Constants

Parameter	Units	Sacramento Delta	Patuxent Estuary	Potomac Estuary	James Estuary	Neuse Estuary
Saturating Light Intensity	langley/day	300	350	300	300	200 * 100 **
Saturated Growth Rate	/day @ 20°C	2.5	2.4	2.0	2.0-2.5	Fig. 9
Endogenous Respiration Rate	/day @ 20°C	0.1	0.125	0.125	0.1	0.1
Death Rate	/day @ 20°C	--	0.125	0.02	0.1	0.05
Settling Velocity	ft/day	--	--	0.3	0.75	1.31* 0.49**
Michaelis Constant (P)	mg/l	--	1.0	1.0	1.0	5.0
Michaelis Constant (N)	mg/l	25.0	5.0	25.0	5.0	25.0 .
Salinity Thresholds	ppt	1.0-4.0	--	--	--	1.0,2.0
Maximum Salinity Effect		0.4	--	--	--	0.4
Carbon/ Chlorophyll	mg/mg	50	50	50	25	50
Nitrogen/ Chlorophyll	mg/mg	7	7	10	7	7
Phosphorus/ Chlorophyll	mg/mg	--	1	1	1	1
Oxygen/ Chlorophyll	mg/mg	--	133	-	66.75	66.75

* diatoms, greens
** blue-greens
. no nitrogen limitation for the nitrogen-fixing blue-greens

Table 5. Nutrient Kinetic Coefficients

Parameter	Units	Sacramento Delta	Patuxent Estuary	Potomac Estuary	James Estuary	Neuse Estuary
Org.N Hydrolysis Rate	/day @ 20°C		0.02	0.075	0.10~ 0.15	0.1
θ for Hydrolysis Rate	unitless		1.045	1.08		1.08
Org.P Hydrolysis Rate	/day @ 20°C		0.02	0.22	0.05~ 0.10	0.1
θ for Hydrolysis Rate	unitless		1.045	1.08		1.08
Nitrification Rate	/day @ 20°C		--	0.09~ 0.13	0.05~ 0.15	0.05

addition, the summer of 1983 was a relatively calm period, making wind-induced reaeration even less important. An average value of 0.5 ft/sec was used for the tidal velocity, based on literature data on the Neuse Estuary (Giese et al., 1985).

Other Model Input

The boundary conditions, initial conditions, and waste loads were directly obtained from the data collected in 1983 and 1984. The freshwater flows were derived from the data collected at the USGS gaging station at Kinston (see Figure 3).

4.2 Model Calibration of 1983 Data

The model was first calibrated using the hydrologic and environmental conditions of 1983. The procedure, as described in the preceeding section, was followed to derive the model input from the 1983 data. The results of modeling analyses are presented in Figures 13 to 16 for Stations 74, 68, 58, and 52, respectively. Only the model results from the surface segments are presented because the bottom segments do not support any significant algal growth. In each figure, a comparison between the observed data and model results is presented for the following water quality parameters: NH_4, NO_2+NO_3, orthophosphate, salinity, total chlorophyll a, and dissolved oxygen. In general, the model results reproduce the observed seasonal trends of all six parameters reasonably well. Some slight differences between the model predictions and observed data for orthophosphate in late 1983 are probably due to the temporal resolution of the upstream boundary conditions (e.g., input is on a 15-day basis). Assigning the boundary conditions on a more frequent basis is expected to improve the model results. Similar observation can be stated for nitrate and dissolved

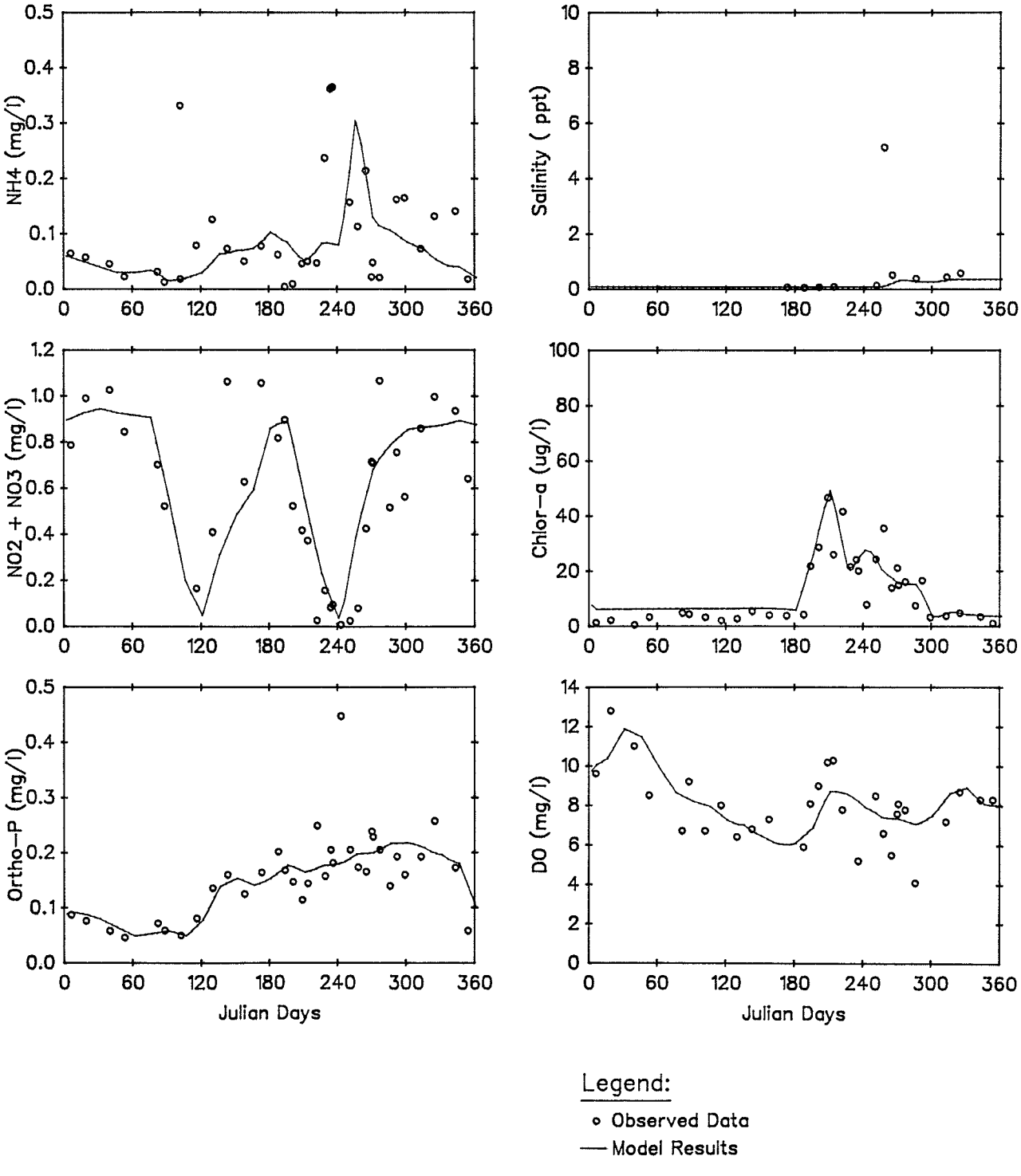

Figure 13. Model Calibration – Station 74, 1983

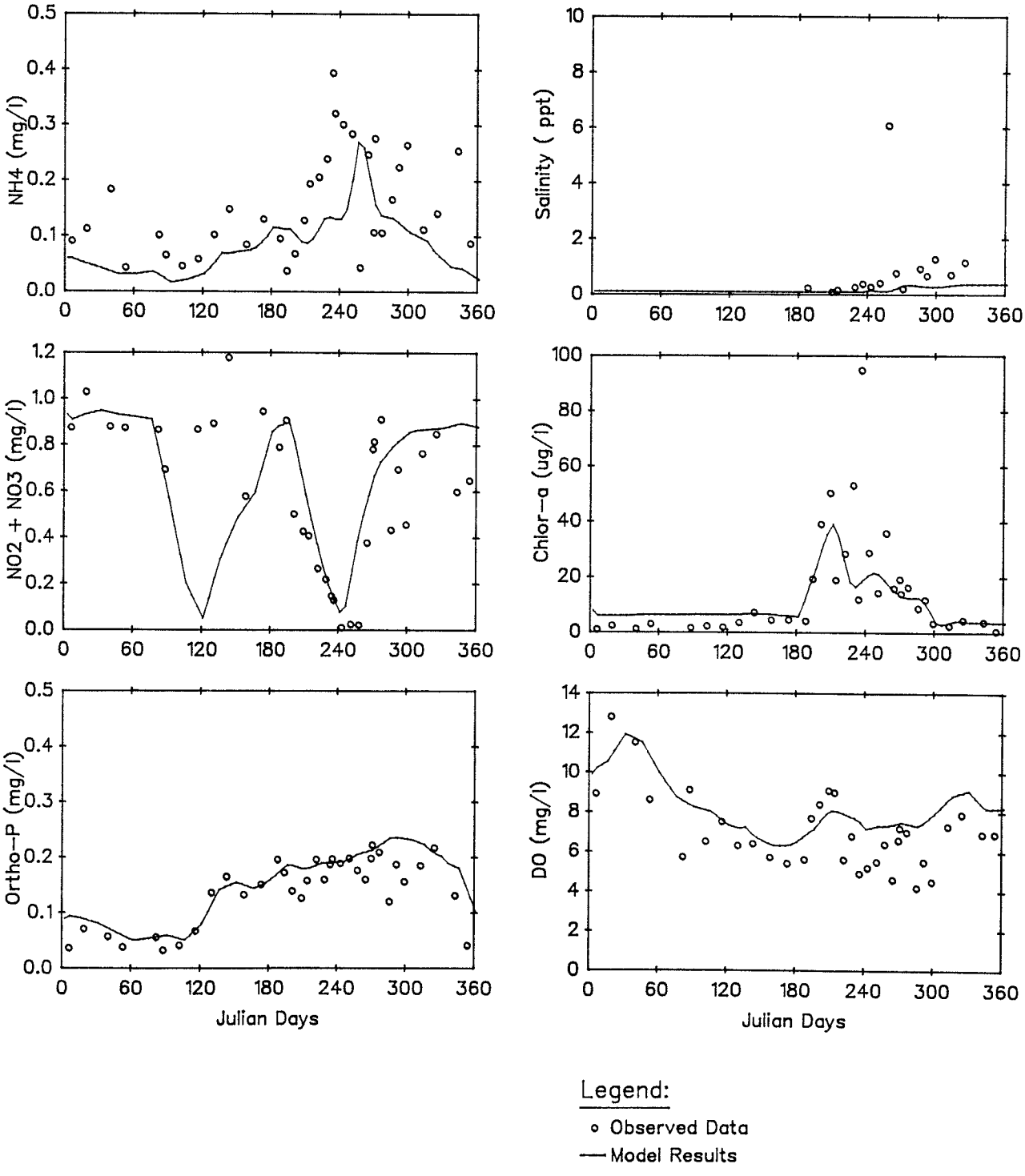

Figure 14. Model Calibration – Station 68, 1983

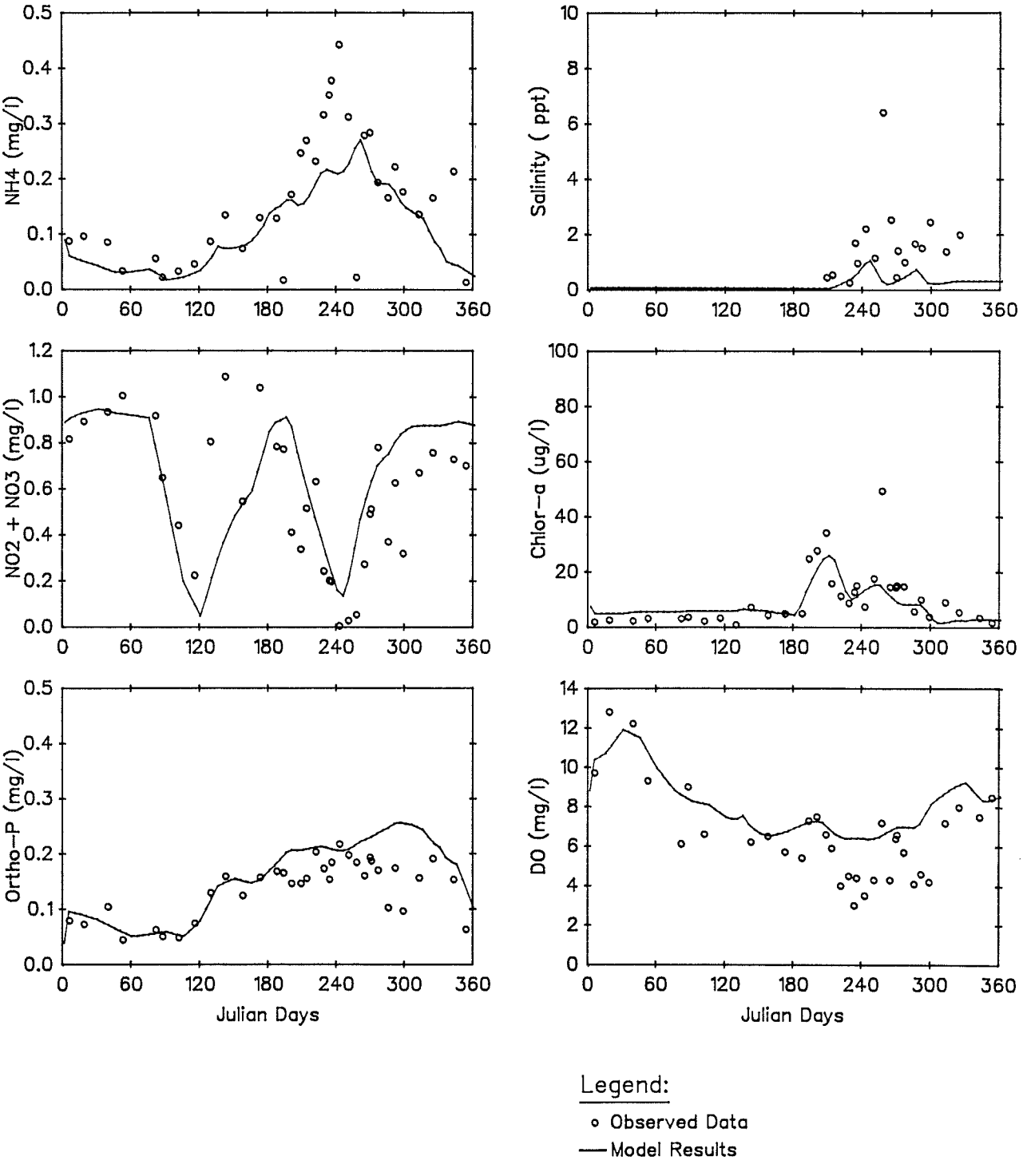

Figure 15. Model Calibration – Station 58, 1983

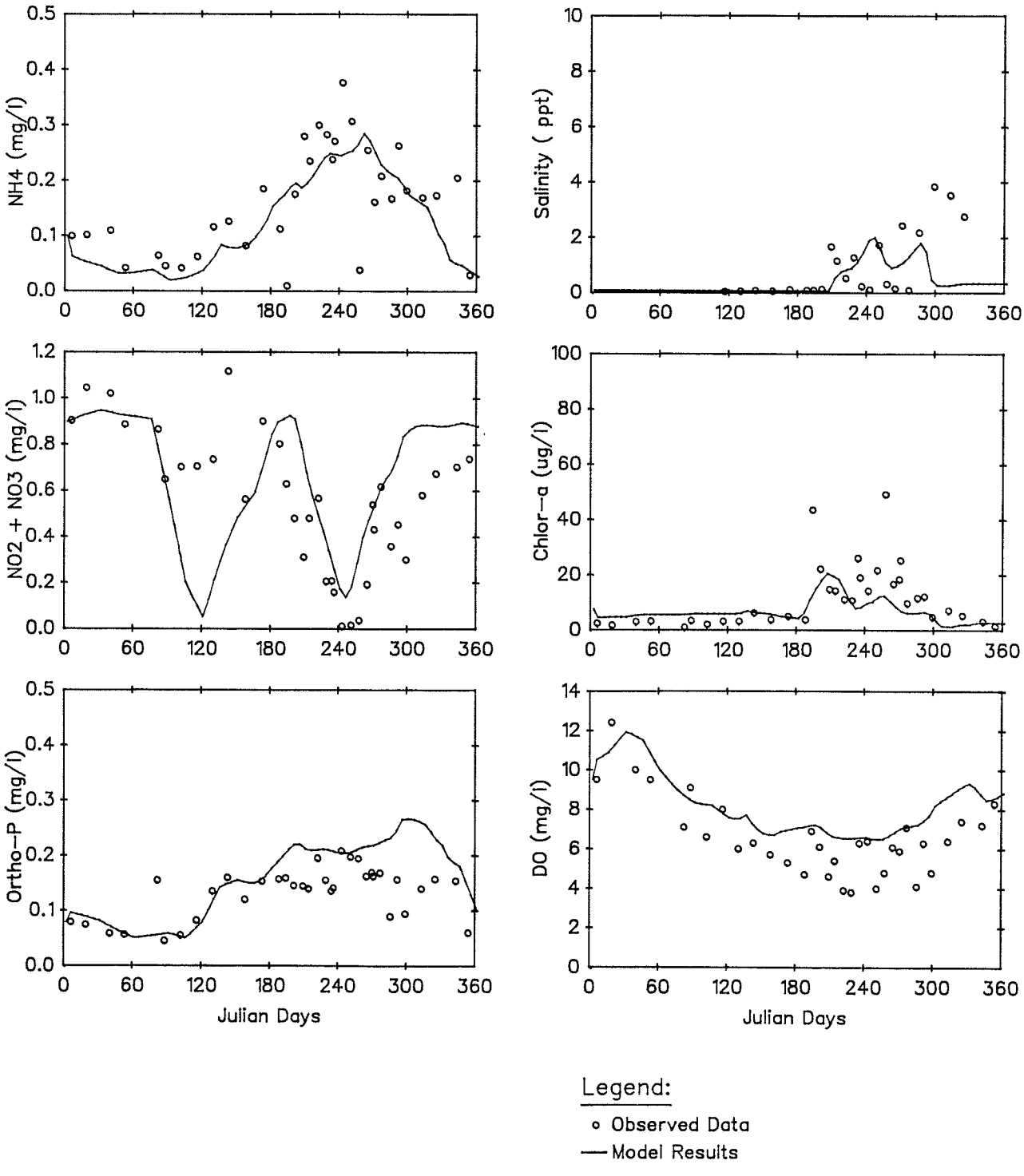

Figure 16. Model Calibration – Station 52, 1983

oxygen in terms of comparing the model results with the data as these two parameters are closely related to watershead runoff on a transient basis.

During the bloom period, nitrate levels reduce significantly while ammonia nitrogen concentrations remain high during the peak of the bloom period. The elevated ammonia levels between Stations 74 and 52 is most likely due to Weyerhauser's input although nitrogen recycling from algal biomass may also contribute to the increase.

The model results show that orthophosphate always in large supply for phytoplankton growth throughout the year. During the bloom period, nitrate levels reduce significantly while ammonia nitrogen concentrations remain high during the peak of the bloom. The two-layer mass transport pattern reproduces the temporal and spatial salinity distributions very well. An increase in salinity in the downstream area (Station 52) beginning around day 195 is reproduced. The elevated salinity levels slightly reduce the phytoplankton growth rate. Both the chlorophyll _a_ and dissolved oxygen calculations match the data closely.

Both the observed data and model results show relatively high levels of dissolved oxygen in the surface layer at the beginning of the year followed by gradual decrease as the temperature increases. This is because the saturation concentration of dissolved oxygen is a factor of temperature and salinity. Further, the increase in the surface dissolved oxygen levels beginning around day 180 is the result of the increase in algal photosynthesis. A quick calculation proves that this is indeed what the model is simulating. Based on an oxygen to chlorophyll _a_ ratio of 66.75 mg O_2/mg Chl used in the model, a net increase in phytoplankton chlorophyll _a_ of 50 µg/l around day 195 (see

Figure 16), therefore results in a production of 3.34 mg/l of dissolved oxygen. The increase in dissolved oxygen calculated by the model at day 195 is quite close to that value.

Figures 17 and 18 show a close comparison between the model calculations and observed data for four different groups of phytoplankton: diatoms, greens, non-nitrogen fixing blue-greens, and nitrogen fixing blue-greens. Both the data and model results indicate that the non-nitrogen fixing blue-green algae are the dominating group. The most abundant blue-green non-nitrogen fixing species found in the lower Neuse in 1983 are Microcystis and Anacystis species (NC Department of Natural Resources, 1984). It can also be noted that the peak in the diatoms occurs in the early spring months. Diatoms do not thrive when the blue-green algae is most abundant, primarily because the blue-greens stay near the surface and reduce the amount of light that is available for the diatoms. The model incorporates this aspect by including the shading of the blue-greens over the diatoms and greens, thereby reducing the available light for these two groups during the blue-green bloom periods.

4.3 Model Calibration of 1984 Data

The Neuse Estuary Eutrophication Model was applied to analyze the 1984 data. This is an interesting test for the model since the 1984 hydrologic conditions are quite different than those exhibited in 1983 (see Figure 3). The most noticeable difference in the hydrologic conditions is the freshwater flow during the summer months. Summer flow was significantly higher in 1984 than 1983. In addition, summer temperature was slightly lower in 1984. As a result, no blue-green bloom occurred in 1984 although the nutrient concentrations were more or

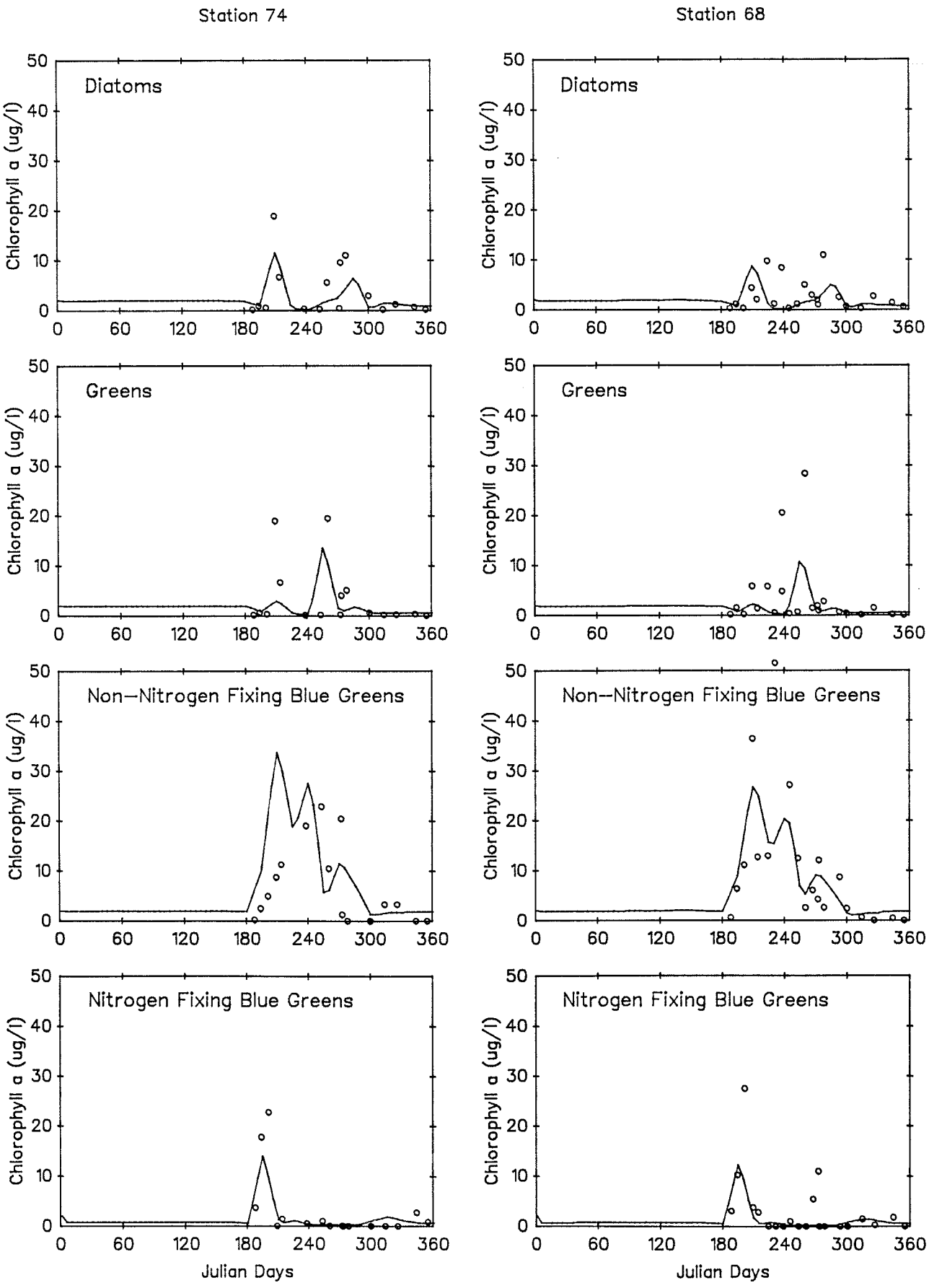

Figure 17. Algal Species Chlorophyll a Calibration — Stations 74 & 68, 1983

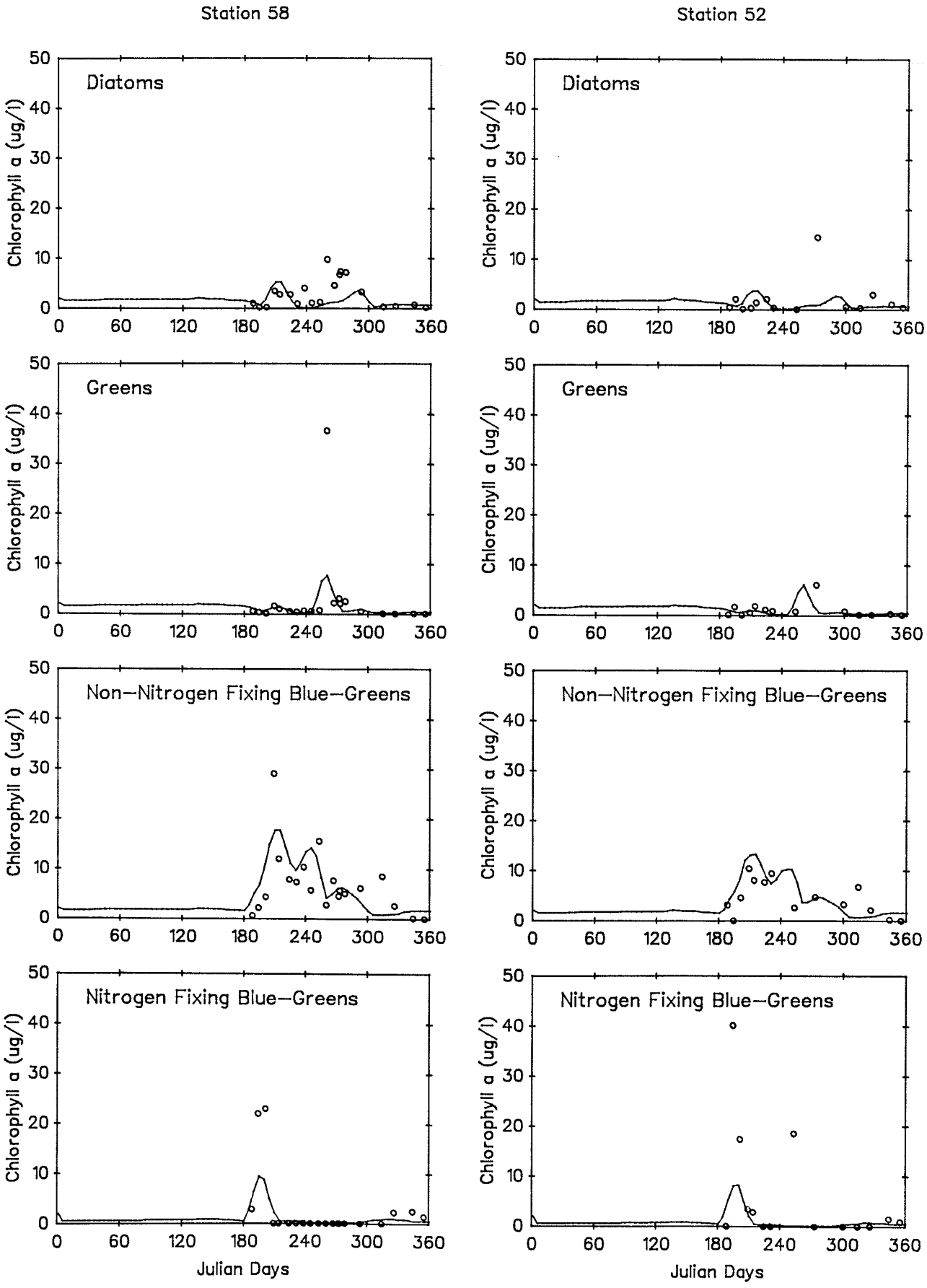

Figure 18. Algal Species Chlorophyll a Calibration – Stations 58 & 52, 1983

less the same levels as those observed in 1983 and the salinity intrusion did not reach the study area in 1984.

The same kinetic constant and coefficient values for the 1983 calibration were used in the model calibration of the 1984 data. Only the exogenous variables such as light extinction coefficient, average daily surface light intensity, temperature, upstream boundary conditions, and the mass transport patterns were changed according to the 1984 conditions. The results of model calculations are presented in Figures 19 to 22. In general, the model results match the observed data reasonably well. Note that the salinity levels in the lower Neuse are relatively low throughout the year due to higher freshwater flows. That is, the salinity intrusion is pushed downstream from the 1983 locations, particularly during the summer months. The model calculations, based on new mass transport patterns (no upestuary flow in the bottom layer), are able to reproduce the salinity distributions. The results for individual phytoplankton functional groups at Stations 52 and 58 are presented in Figure 23. It is seen that the blue-greens, particularly the nitrogen fixing species, are noticeably less significant (as a biomass fraction) in 1984 than 1983.

4.4 Factors Limiting Algal Growth in the Lower Neuse River

The 1983 results are further examined to determine the limiting factors on algal growth in the lower Neuse River. The model results (see Figures 13 and 16) show that nutrient concentrations are sufficient for phytoplankton growth at the beginning of the bloom. However, nitrogen proved to be limiting in 1983 once the bloom became firmly established. On the other hand, light effect on algal growth is rather significant during most of the year, reaching almost an 80% reduction in

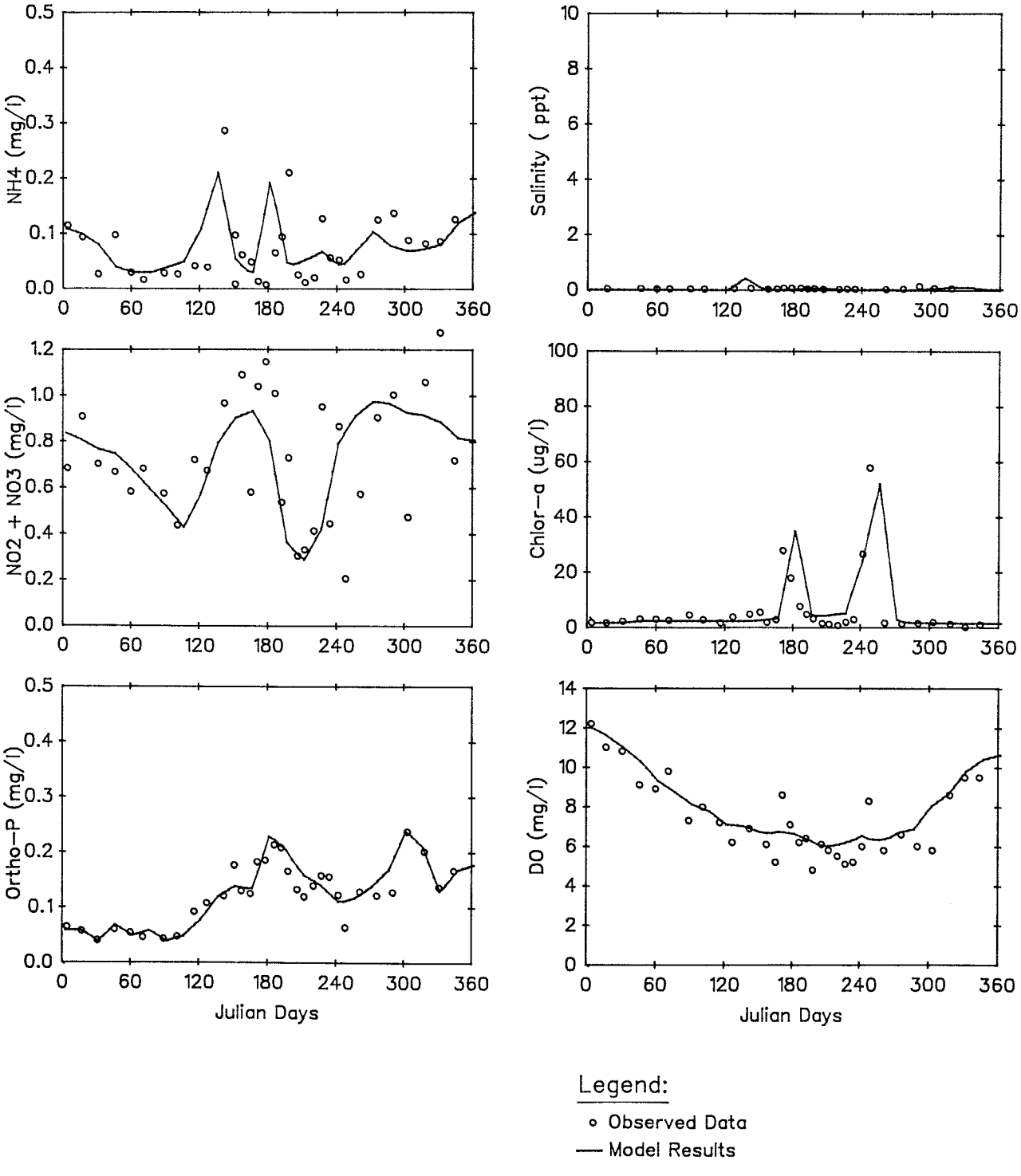

Figure 19. Model Calibration – Station 74, 1984

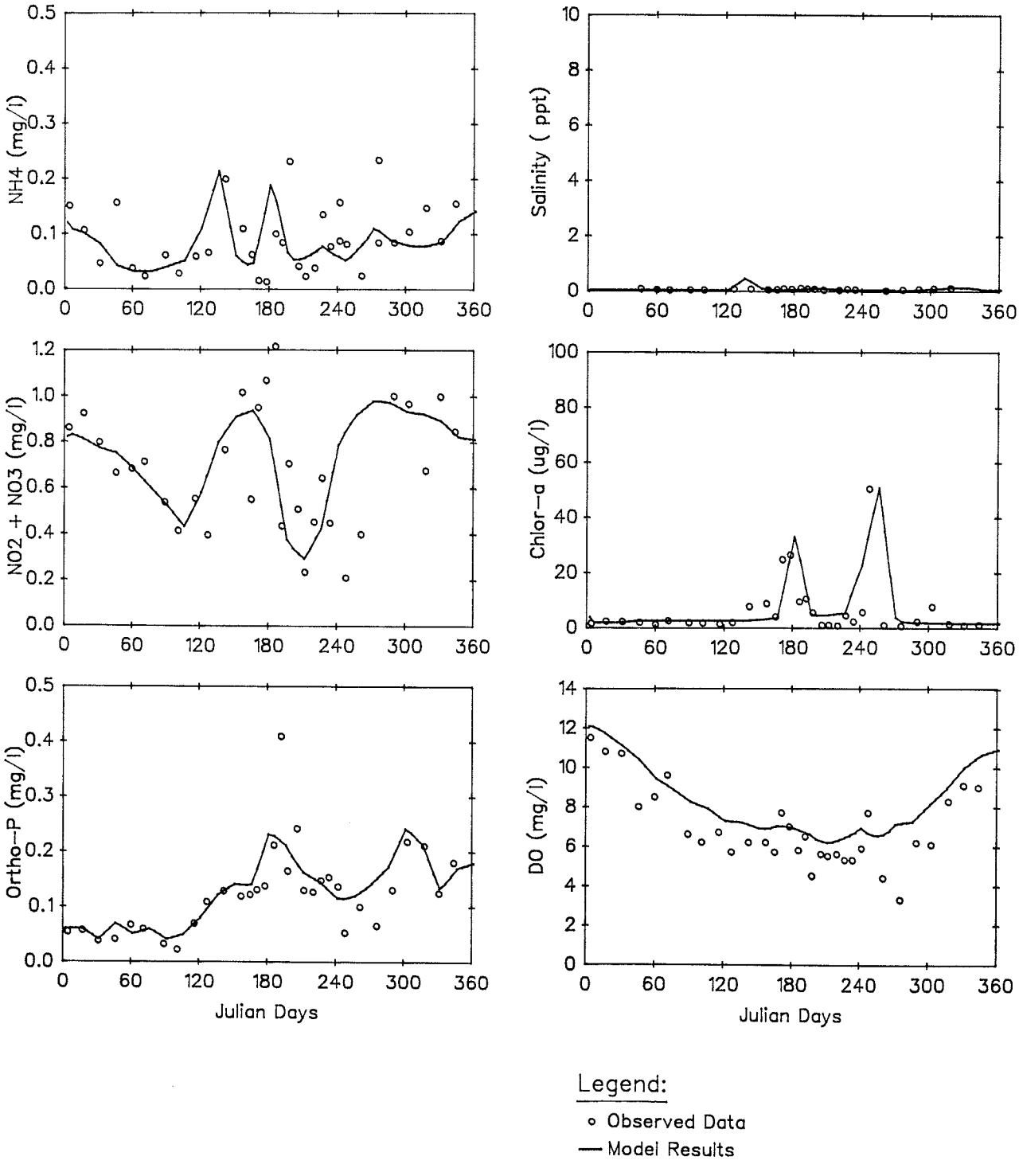

Figure 20. Model Calibration – Station 68, 1984

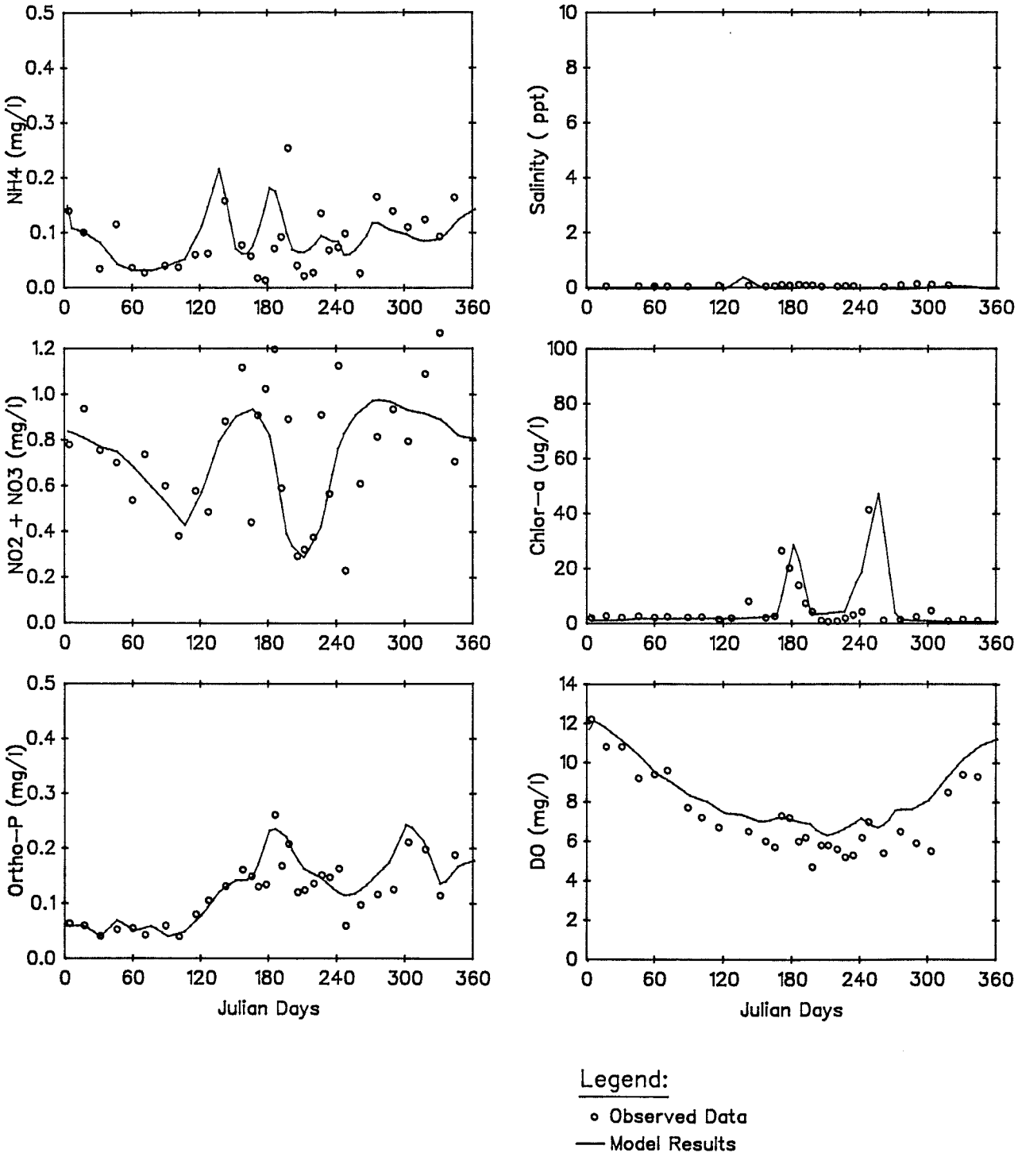

Figure 21. Model Calibration – Station 58, 1984

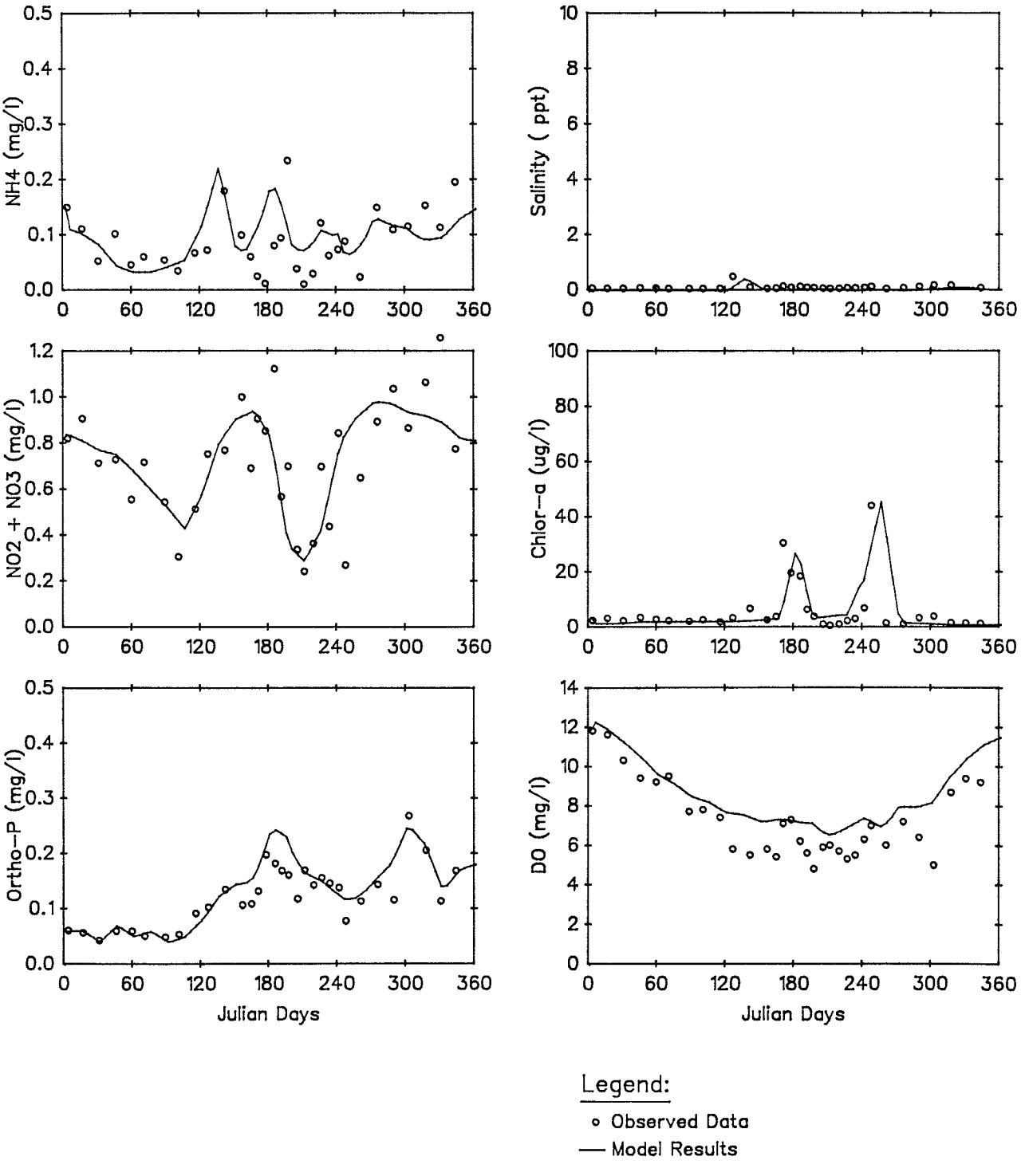

Figure 22. Model Calibration – Station 52, 1984

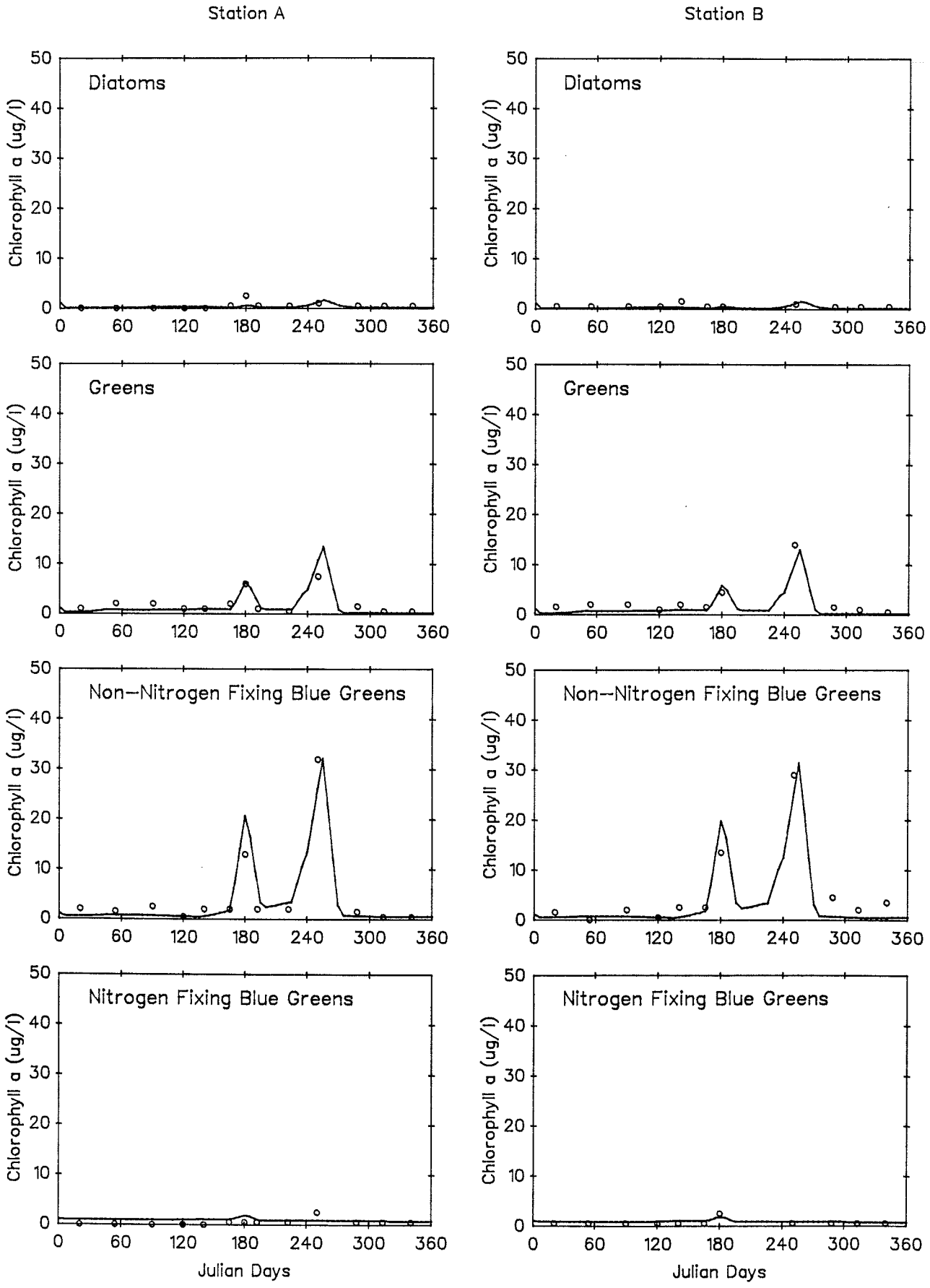

Figure 23. Algal Species Chlorophyll a Calibration, 1984

growth rate (Figure 24). During the summer months of 1983, salinity intrusions reached the bloom area and had a moderate impact on algal growth rate (Figure 24).

4.5 Model Sensitivity Analyses

By examining a model's responses to changes in certain key parameters, a sensitivity analysis would provide additional insights into the phytoplankton-nutrient dynamics. It is especially important to examine the model kinetic coefficients and parameters that are uncertain and difficult to quantify independently. Since nutrients are usually in sufficient supply for algal growth in the lower Neuse, the sensitivity analyses focus on other parameters associated with phytoplankton growth and death. The 1983 calibration was used as a basis in the sensitivity analyses.

The phytoplankton endogenous respiration rate is estimated for the model input as 0.1/day based on literature values (Table 4). The model was run using a reported range from 0.08/day to 0.125/day (O'Connor et al., 1975). The model results indicate that there is no significant change in any of the system variables modeled. The model is not sensitive to the variation of algal endogenous respiration rates in terms of phytoplankton biomass and dissolved oxygen. Thus, the value used for all four phytoplankton groups in the model calibration (0.1/day) is considered acceptable to the analysis.

The non-predatory death rate of phytoplankton ranged in the literature from 0.02/day to 0.1/day (O'Connor et al., 1975). The phytoplankton biomass involved in non-predatory death are available for recycling (of nutrients) within the system. The model calibration uses

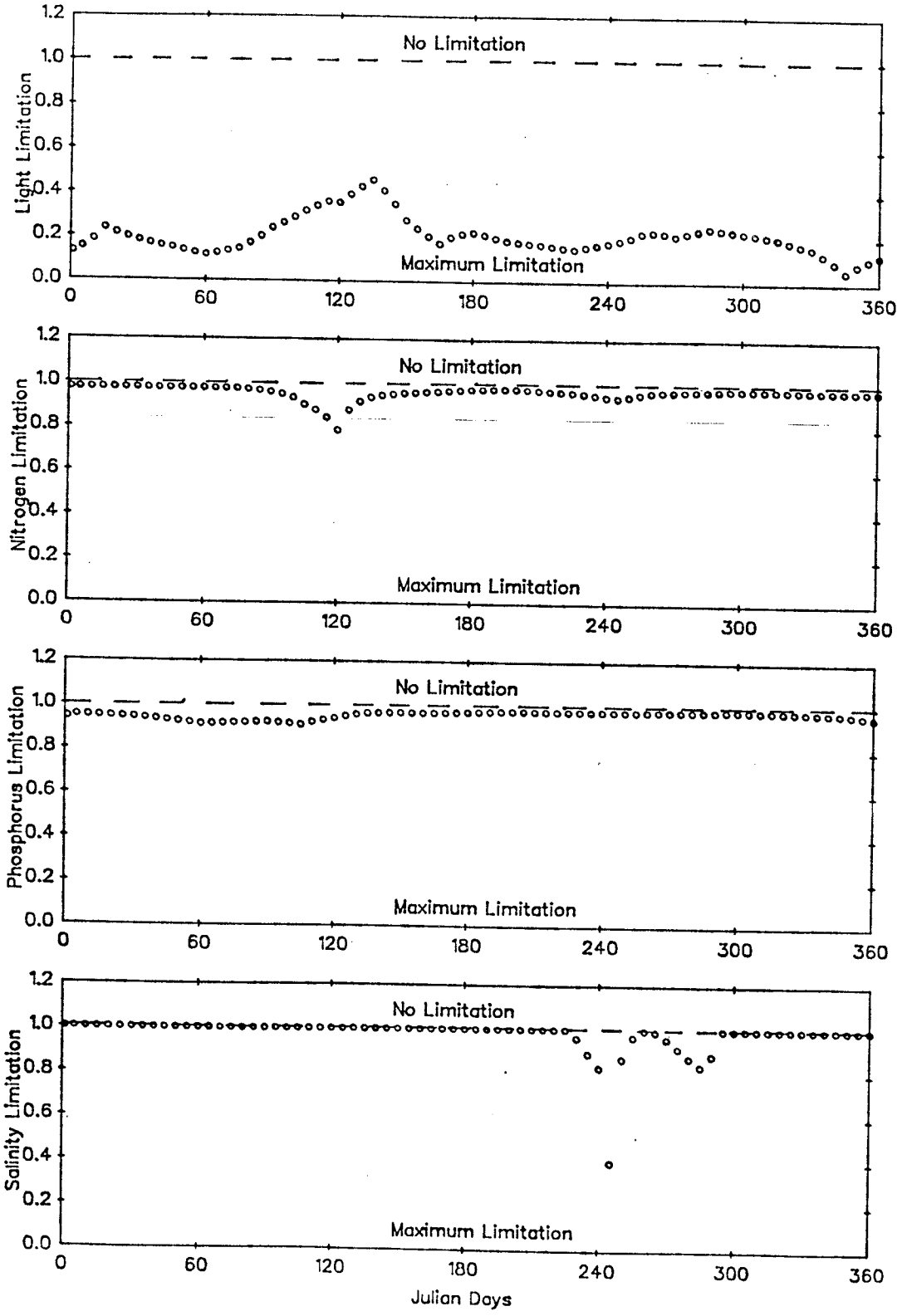

Figure 24. Growth Limitation, Non–Nitrogen Fixing Blue Greens, 1983

a value of 0.05/day for the lower Neuse. Again, model sensitivity analysis of the death rate show no significant changes in the model results resulting from the variation of the algal death rate.

As indicated in earlier discussions, the light extinction coefficient (K_e) is an important parameter. K_e is input into the model as a time-variable function throughout the year and is derived from measured light intensity data. Figure 25 shows the results of the sensitivity analysis. It can be seen that although an increase in K_e by 50% gives a better fit for the ammonia data, the chlorophyll *a* fit is not good. To reproduce all system variables reasonably well, the K_e values used in the model calibration appear to be most appropriate.

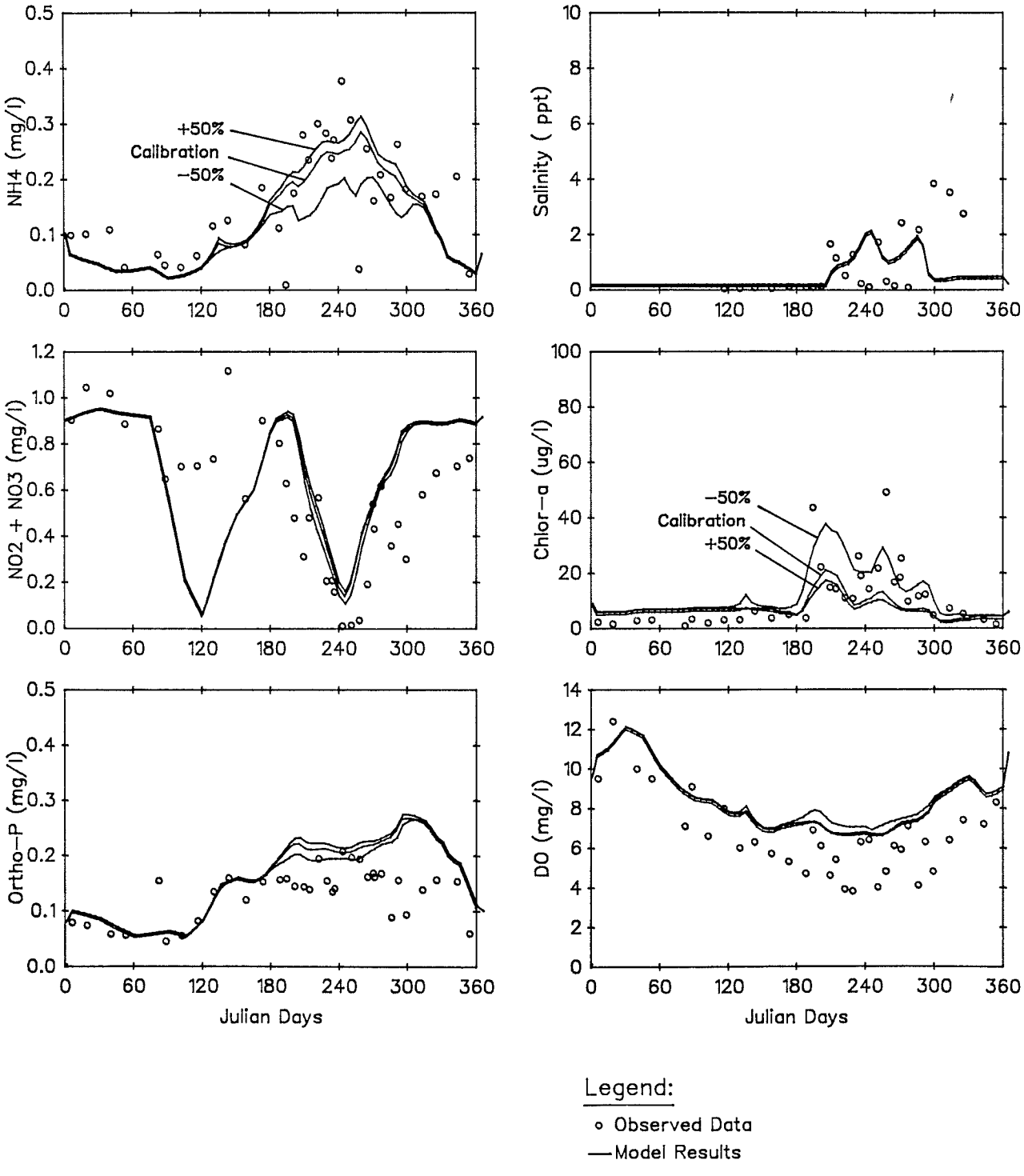

Figure 25. Model Sensitivity Analysis – Light Extinction Coefficient

5. DISCUSSIONS

5.1 Hypothesis of Blue-Green Bloom Potential

The model calibration results are consistent with a hypothesis for the blue-green algae in the Neuse River. That is, the blue-green algal blooms are strongly regulated by the nutrient supply from the spring months as well as the river flow condition in the summer months. In 1983, relatively high runoff in spring and warm temperatures/low flows in the summer months produced an intensive Microcystis bloom. On the other hand, the summer months in 1984 were wet although the spring flows in 1984 were about the same as those in the spring of 1983. As a result of the relatively high flows in the summer months, no significant Microcystis bloom was observed in the lower Neuse in 1984. The Neuse Estuary Eutrophication Model (NEEM) is able to mimic these observed trends reasonably well.

The 1985 condition is different from the 1983 and 1984 conditions in that a dry spring and a moderately wet summer were observed in the Neuse River watershed during the year. As a result, no Microcystis bloom has been observed to date. Thus, it is interesting to see whether NEEM would reproduce the observed 1985 results as well. A successful reproduction of the 1985 water quality data would further validate the above hypothesis and the modeling framework and would provide additional confidence in the model.

5.2 Upstream Boundary Conditions

The Neuse Estuary Eutrophication Model (NEEM) is able to reproduce the 1983 and 1984 data in a "reasonable" fashion. It should be stressed that there are many model coefficients and parameters which values must be assigned prior to running the model. One of the most important

parameters is the upstream boundary condition which supplies the nutrient loads and freshwater discharges into the study area and thereby has significant bearings on the model response. Further, the upstream boundary condition becomes particularly important in model projection analyses of assessing the system responses to various management alternatives. Many management alternatives may involve changes in the upper watershed of the Neuse. Thus, there is a need to accurately quantify the upstream boundary condition (an exogenous model parameter) of NEEM by relating the nutrient input from the upper basin with the fate and transport of the nutrients in the riverine portion of the Neuse.

One of the tasks of this study was analyzing the fate and transport in the riverine system of the Neuse River. Examination of the available water quality data for the riverine portion does not suggest any elaborate modeling exercise (i.e., like NEEM). The most comprehensive data base at the time of this study consists of the water quality data from surveys in 1979. Although the Department of Natural Resources conducted intensive water quality surveys (including time-of-travel surveys) during the summer months of 1985, the complete data was not available for this study. Thus, the 1979 data was used for a riverine fate and transport analysis, using a steady-state one-dimensional model framework which kinetics structure is similar to the James River Model (Lung, 1985, 1986).

The results of the fate and transport analysis are presented in Figures 26 and 27 for the 1979 summer and spring conditions, respectively. The calculation results show that the nutrient concentrations are not significantly attenuated between Raleigh and

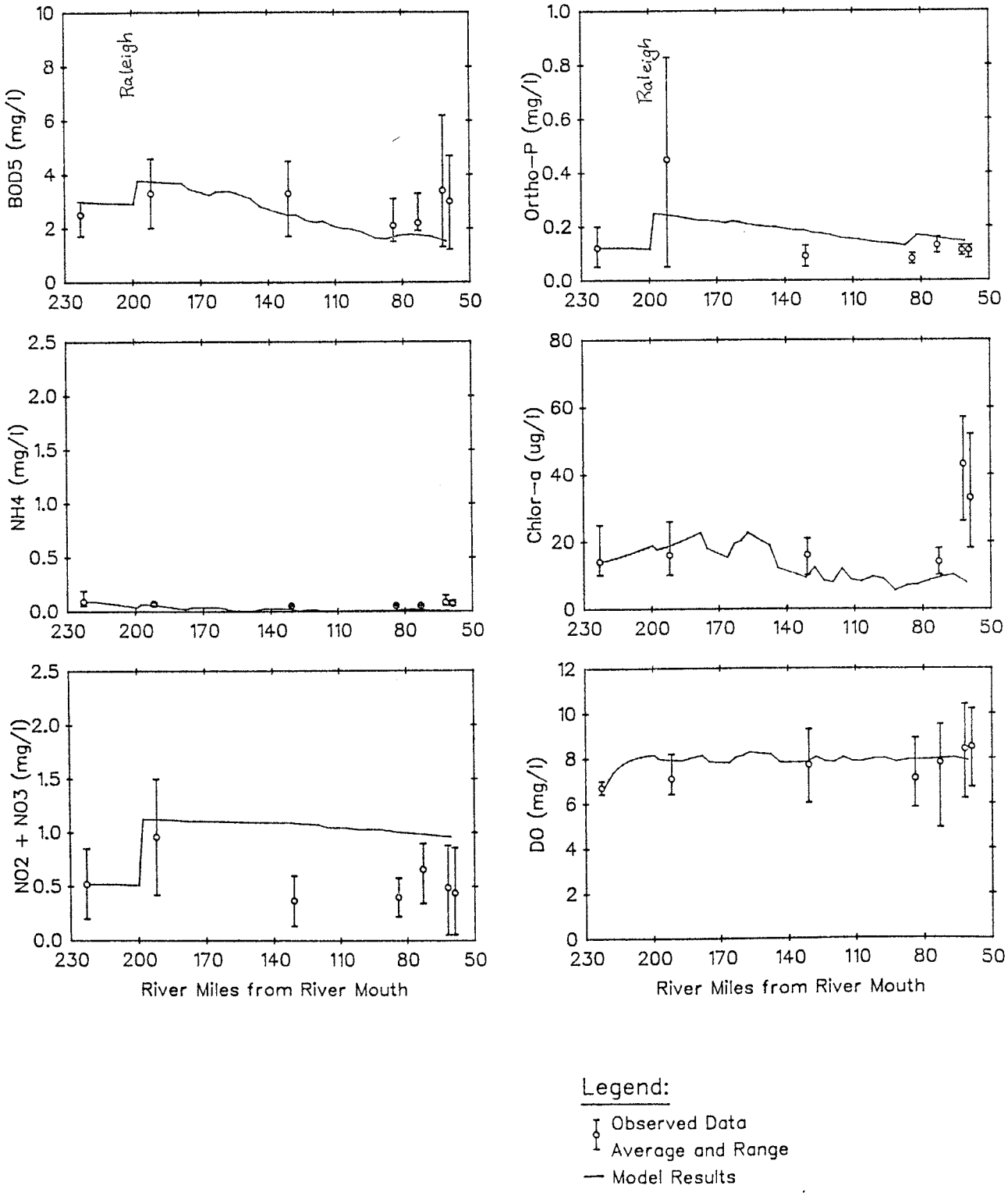

Figure 26. Water Quality Modeling of Neuse River (Summer 1979)

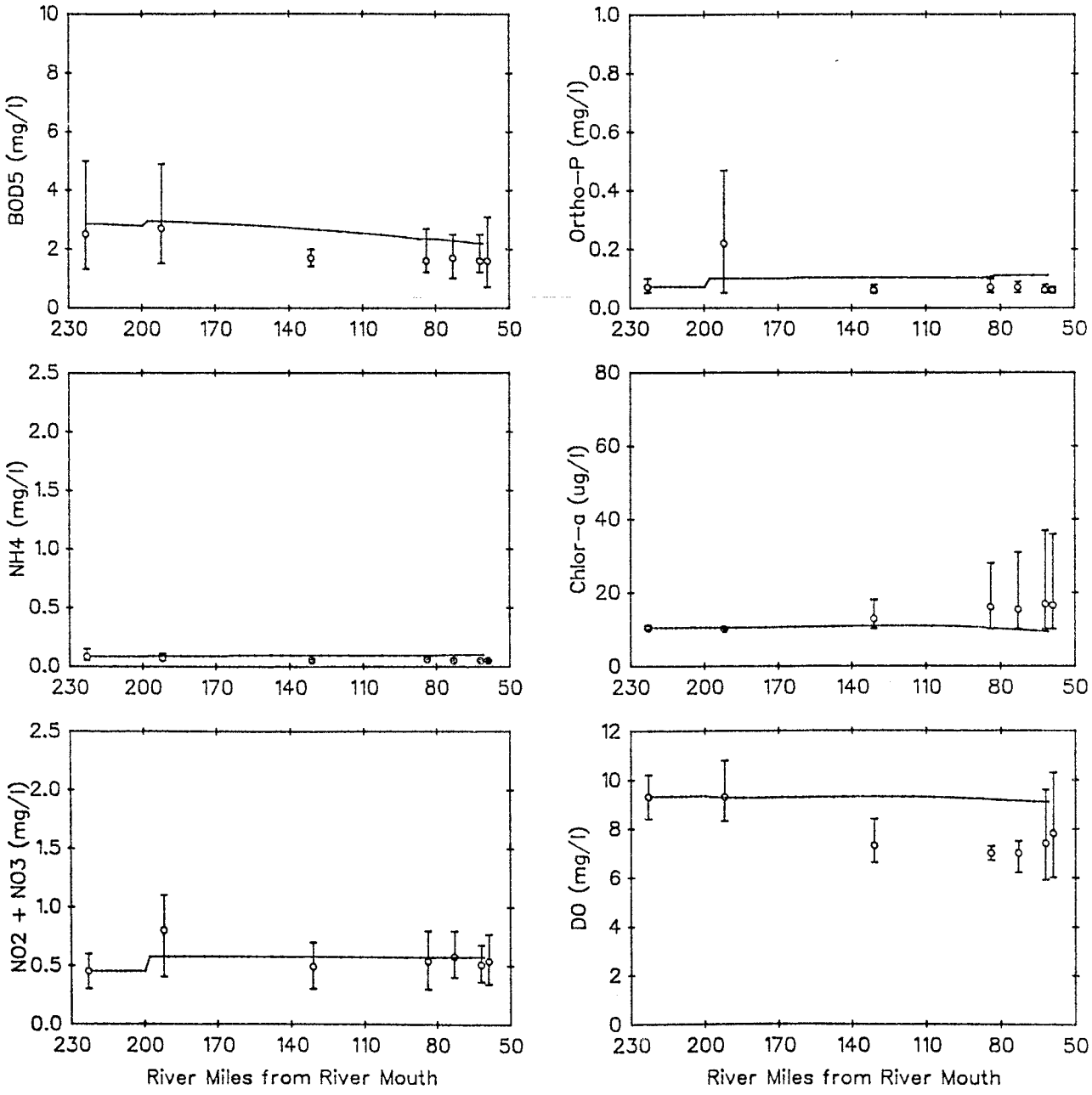

Figure 27. Water Quality Modeling of Neuse River (Spring 1979)

Kinston. However, the data indicates that the downstream concentrations of chlorophyll a increase sharply while the model results deviate from the chlorophyll a data significantly. Due to the lack of spatial resolution (in longitudinal direction) of the data, a significant degree of uncertainty exists for the chlorophyll a concentrations at the downstream location. Nevertheless, the preliminary results indicate that the riverine fate and transport analysis can be used to quantify the fate and transport of the nutrients in the Neuse River. It is expected that the coefficients of the riverine model can be refined using the 1985 data (available from the Department of Natural Resources soon).

5.3 Future Model Improvement

The Neuse Estuary Eutrophication Model has been developed utilizing the data currently available. Following the model calibration analysis of the 1983 and 1984 data, a number of areas have been identified for future model improvement in order to better address the impact of nutrient control on algal growth. First, it is highly possible that nutrients stored in the lower Neuse River sediments may become available for algal growth once the external supply of nutrients is reduced. The model may be modified to incorporate nutrient release from sediments. At the present time, however, data on sediments in the lower Neuse is limited. A good understanding of sediments is needed before such a model enhancement could be implemented. Second, dissolved inorganic carbon may be incorporated as a state variable to characterize the buoyancy mechanism for blue-green algae as well as to address carbon limitation on algal growth.

REFERENCES

Auer, M. T., and R. P. Canale, 1980. Phosphorus Uptake Dynamics as Related to Mathematical Modeling at a Site on Lake Huron. Journal of Great Lakes Research, Vol. 6, No.1, pp. 1-7.

Booker, M. J. and A. E. Walsby, 1982. Bloom Formation and Stratification by a Planktonic Blue-Green Alga in an Experimental Water Column. British Phycological Journal, Vol. 16, pp. 1-11.

Canale, R. P., and A. H. Vogel, 1974. Effects of Temperature on Phytoplankton Growth. ASCE Journal of the Environmental Engineering Division. Vol. 100, No. EE1, pp. 231241.

Christian, R. R., and D. W. Stanley, 1984. Microbiological Changes Occurring at the Freshwater-Seawater Interface of the Neuse River Estuary, North Carolina. In The Estuary as a Filter, V. S. Kennedy, ed., Academic Press, pp. 349-365.

Di Toro, D. M., D. J. O'Connor, and R. V. Thomann, 1971. A Dynamic Model of the phytoplankton Population in the Sacramento San Joaquin Delta. Adv. Chem. Ser. 106, Am. Chem. Soc., pp. 131-180.

Di Toro, D. M., J. J. Fitzpatrick, and R. V. Thomann, 1980. Water Quality Analysis Simulation Program (WASP) and Model Verification Program (MVP) Documentation. Prepared for the U.S. EPA, Grosse Ile Laboratory, NERC, Grosse Ile, Michigan.

Filardo, M. J., 1984. Phytoplankton Ecology and Dynamics in the James River Estuary, Virginia, U.S.A. PhD Dissertation submitted to the Old Dominion University in partial fulfillment of the requirements for the Degree of Doctor of Philosophy, 201 pp.

Giese, G. L., H. B. Wilder, and G. G. Parker, Jr., 1985. Hydrology of Major Estuaries and Sounds of North Carolina. USGS Water Supply Paper 2221, 108 pp.

HydroQual, 1981. Water Quality Analysis of the Patuxent River. Report prepared for the State of Maryland.

Lung, W. S., 1985. Assessing the Water Quality Benefit of Point Source Phosphorus Control in the James River Basin. Report No. UVA/532533/CE85/101, University of Virginia, Department of Civil Engineering prepared for the Soap and Detergent Association, 60 p.

Lung, W. S., 1986. Assessing Phosphorus Control in the James River Basin, ASCE Journal of Environmental Engineering Division, Vol. 112, No. 1, pp. 44-60.

Lung, W. S., and D. J. O'Connor, 1978. Assessment of the Effects of Proposed Submerged Sill on the Water Quality of Western Delta-Suisun Bay. Submitted by Hydroscience to U.S. Army Corps of Engineers, Sacramento, CA, 140 p.

Lung, W. S., and D. J. O'Connor, 1984. Two-Dimensional Mass Transport in Estuaries. ASCE Journal of Hydraulic Engineering Division, Vol. 110, No. 10, pp. 1340-1357.

Mitchell, S., 1985. N.C. Department of Natural Resources, personal communication.

Morris, A. W., A. J. Bale, and R. J. M. Howland, 1982. Chemical Variability in the Tamar Estuary South-West England. Estuarine Coastal and Shelf Science, Vol. 14, pp. 649-661.

NC Department of Natural Resources, 1984. 1983 Neuse River Phytoplankton Summary. Report No. 84-06, 40 pp.

O'Connor, D. J., D. M. Di Toro, and R. V. Thomann, 1975. Phytoplankton Models and Eutrophication Problems. In Ecological Modeling, Clifford S. Russel, ed., Resources for Future, Inc., Washington, DC, pp. 149-208.

O'Connor, D. J., and W. S. Lung, 1981. Suspended Solids Analysis of Estuarine Systems. ASCE Journal of Environmental Engineering Division, Vol. 107, No. EE1, pp. 101-120.

Paerl, H. W., 1983. Factors Regulating Nuisance Blue-Green Algal Bloom Potentials in the Lower Neuse River, NC. University of North Carolina Water Resources Research Institute Report 83-188, 48 p.

Paerl, H. W., 1986. Nuisance Algal Bloom in Lakes, Rivers, and Coastal Marine Waters. In Comparative Ecology of Freshwater and Coastal Marine Ecosystems, S. W. Nixon, ed., Proceedings of the UNISCO Symposium held in Nairobi, 1985.

Paerl, H. W., P. T. Bland, J. H. Blackwell, and N. D. Bowlés, 1984. The Effects of Salinity on the Potential of Blue-Green Algal (Microcystis aeroginosa) Bloom in the Neuse River Estuary, NC. Institute of Marine Science, University of North Carolina Working Paper 84-1.

Paerl, H. W. and J. F. Ustach, 1982. Blue-Green Algal Scums: An Example for the Occurrence During Freshwater Blooms. Limnol. Oceanogr., Vol. 27, No. 2, pp. 212-217.

Pennock, J. R., 1983. Regulation of Chlorophyll Distribution in the Delaware Estuary by Short Term Variability in Vertical Stratification and Suspended Sediment Concentration. EOS Transactions, American Geophysical Union, Vol. 64, No. 52, p. 1041.

Sharp, J. H., C. H. Sulberson, and T. M. Church, 1982. The Chemistry of the Delaware Estuary. General Considerations. Limnol. and Oceanogr., Vol. 27, No. 6, pp. 1015-1028.

Stanley, D. W., 1983. Nutrient Cycling and Phytoplankton Growth in the Neuse River. Final Report prepared for the UNC Water Resources Research Institute. Report No. 204, 85 pp.

Stanley, D. W., and R. R. Christian, 1984. Nutrients in Estuaries: Research Needs and Priorities. In Research for Managing the Nation's Estuaries: Proceedings of a Conference in Raleigh, North Carolina, March 13-15, 1984. UNC Sea Grant College Publication UNC-SG-84-08, pp. 203-217.

Tedder, S. W., J. Sauber, L. Ausley, and S. Mitchell, 1980. Working Paper: Neuse River Investigation, 1979. North Carolina Department of Natural Resources and Community Development, Division of Environmental Management.

Thomann, R. V., D. M. Di Toro, and D. J. O'Connor, 1974. Preliminary Model of Potomac Estuary Phytoplankton. ASCE Journal of Environmental Engineering Division, Vol. 100, No. EE2, pp. 699-715.

Thomann, R. V., R. P. Winfield, and J. J. Segna, 1979. Verification Analysis of Lake Ontario and Rochester Embayment Three Dimensional Eutrophication Models. Prepared for the EPA, 600/3-79-094, p. 100.

Thomann, R. V., and J. J. Fitzpatrick, 1982. Calibration and Verification of a Mathematical Model of the Eutrophication of the Potomac Estuary. Prepared by HydroQual, Inc., for the Government of the District of Columbia, 484 pp.

APPENDIX - Conservation of Mass

The framework of the analysis detailed in this report is based upon the principle of conservation of mass. Simply stated the conservation of mass accounts for all of a material entering or leaving a body of water, transport of material within the water body, and physical, chemical, and biological transformations of the material. Considering an infinitesimal volume oriented along the axis of a three-dimensional coordinate system, a mathematical formulation of the conservation of mass may be written:

$$\frac{\partial c}{\partial t} = \frac{\partial}{\partial x}\left(E_x \frac{\partial c}{\partial x}\right) + \frac{\partial}{\partial y}\left(E_y \frac{\partial c}{\partial y}\right) + \frac{\partial}{\partial z}\left(E_z \frac{\partial c}{\partial z}\right) - \frac{\partial}{\partial x} U_x c - \frac{\partial}{\partial y} U_y c - \frac{\partial}{\partial z} U_z c$$

dispersive transport — advective transport

$$\pm S(x,y,z,t) + W(x,y,z,t)$$

sources or sinks — external inputs

where

- c = concentration of the water quality variable, $[M/L^3]$
- t = time, $[T]$
- E = dispersion (mixing) coefficient due to tides and density and velocity gradients (or diffusion coefficient in the sediment interstitial waters), $[L^2/T]$
- U = net advective velocity, $[L/T]$
- S = sources and sinks of the water quality variable, representing kinetic interactions, $[M/L^3\text{-}T]$
- W = external inputs of the variable c, $[M/T]$
- x,y,z, = longitudinal, lateral and vertical coordinates, respectively, $[L]$

```
C
C*************************************************************************
C
C                        N E U S E
C
C    E U T R O P H I C A T I O N   M O D E L
C
C*************************************************************************
C
C  AUG. 1985
C
C
C  SYSTEMS:
C
C  1. Diatoms                                  mg chl-a/l
C  2. Green Algae                              mg chl-a/l
C  3. Blue-green non-nitrogen fixing           mg chl-a/l
C  4. Blue-green nitrogen fixing               mg chl-a/l
C  5. Organic Nitrogen                         mg N/l
C  6. Ammonia (NH3)                            mg N/l
C  7. NO2 + NO3                                mg N/l
C  8. Organic Phosphorus                       mg P/l
C  9. Ortho-P                                  mg P/l
C 10. Salinity                                 ppt
C 11. Dissolved Oxygen                         mg/l
C
C
C
C_________________________________________________________________________
C
C
C
C  CONSTANTS:
C
C  KMPD       Half saturation constant for phosphorus, diatoms        (mgP/l)
C  KMPG       Half saturation constant for phosphorus, greens
C  KMPB1      Half saturation constant for phosphorus, non-N fixing blue greens
C  KMPB2      Half saturation constant for phosphorus, N fixing blue green
C  ISD..B2    Saturation light intensity for each group               (ly/day)
C  KMND..B1   Half saturation constant for nitrogen for each group    (mgN/l)
C  KRD..B2    Endogenous respiration rate at 20 deg C, for each group (/day)
C  KRTD..B2    temperature coefficient
C  KDRD..B2   Non-predatory death rate                                (/day)
C  SVD..B2    Settling velocity for each type of phytoplankton        (ft/day)
C  S1D..B2    Salinity thresholds for algal growth                    ppt
C  S2D..B2       ''       ''      ''   ''    ''                       ''
C  MINPD..B2  Minimum percent of growth rate for salinity curve
C  DEADD..B2  Fraction of dead cells that drop to bottom
C  CCHLD..B2  Carbon to chl-a ratio
C  NCHLD..B1  Nitrogen to chl-a ratio
C  PCHLD..B2  Phosphorus to chl-a ratio
C  OCHLD..B2  Oxygen to chl-a ratio
C  CHLCD      Chl-a to carbon ratio, diatoms
C  CHLCG      Chl-a to carbon ratio, greens
C  K34        Hydrolysis rate                                         (/day)
```

```
C  K34T        temperature coefficient
C  K45         Nitrification rate                                    (/day)
C  K45T        temperature coefficient
C  K67         Phosphorus to Ortho-p conversion rate                 (/day)
C  K67T        temperature coefficient
C  KBN20       Benthic uptake rate at 20 deg C                      (gm/m2/day)
C
C
C
C
C-------------------------------------------------------------------------------
C
C
C  PARAMETERS:
C
C  DEPTH       Depth of segment                          (feet)
C  VELSG       Avg. tidal and freshwater velocity        (ft/s)
C
C
C
C-------------------------------------------------------------------------------
C
C
C   TIME VARIABLE FUNCTIONS:
C
C   TEMP(1)    Temperature in surface layer              (deg C)
C   TEMP(2)    Temperature in bottom layer               (deg C)
C   IAV        Surface light intensity                   (ly/day)
C   F          Fraction of daylight
C   KE         Light extinction coefficient              (/foot)
C   WIND       Wind velocity                             (meters/s)
C
C
C
C-------------------------------------------------------------------------------
C
C
C
      SUBROUTINE WASPB
      LOGICAL  TOPSEG
      REAL     KMND,ISD,KMPD,KRD,KRTD,KDRD,MINPD,NCHLD,KMSID,KMNG,ISG
      REAL     TEMP(2), DEPTH(12), VELSG(12)
      REAL     NITD,NITG,NITB1,NITB2,NUTD,NUTG,NUTB1,NUTB2
      REAL     T1D,T2D,T1G,T2G,T1B1,T1B2,T2B1,T2B2
      REAL     IAV,KE,KED,KEG,KEBG,KA,KA20,KBNTH
C
C
      REAL   NVOLT,NRT,NQT,NBCT(19),NWKT(19),NFUNT
      REAL   MVOL(120),MR(250),MQ(250),MBC(19,20),MWK(19,80),MFUNC(20)
      INTEGER   OUT,SYSBY(19),RBY(19),QBY(19)
      COMMON   IN,OUT,NOSYS,NOSEG,ISYS,ISEG,ISIM,LISTG,LISTC
      COMMON   INITB,IPRNT,IDUMP(8,2),IDISK,IREC,MXDMP,IDFRC(19)
      COMMON   NBCPSY,NWKPSY,SYSBY,RBY,QBY,NEGSLN
      COMMON   TIME,DT,TZERO,SCALT,TEND,PRNT
      COMMON   OMEGA,ITCHCK,MXITER
      COMMON   C(19,120),CD(19,120),CMAX(19),CMIN(19)
      COMMON   PARAM(120,10),CONST(100)
```

```
      COMMON   BVOL(120),BR(250),BQ(250),BBC(19,20),BWK(19,80),BFUNC(20)
      COMMON   MVOL,MR,MQ,MBC,MWK,MFUNC
      COMMON   IR(250),JR(250),IQ(250),JQ(250),IBC(19,20),IWK(19,80)
      COMMON   IVOPT,NOV,IROPT,NOR,IQOPT,NOQ,IBCOP(19),NOBC(19)
      COMMON   IWKOP(19),NOWK(19),NOPAM,NCONS,NFUNC
      COMMON   NVOLT,NRT,NQT,NBCT,NWKT,NFUNT
      COMMON   ITIMV,ITIMR,ITIMQ,ITIMF,ITIMB(19),ITIMW(19)
C
C
      EQUIVALENCE  (CONST(1),KMND) , (CONST(2),ISD)
      EQUIVALENCE   (CONST(17),KMNG) , (CONST(18),ISG)
      EQUIVALENCE  (CONST(33),KMNB1),(CONST(34),ISB1)
      EQUIVALENCE   (CONST(48),ISB2),(CONST(49),KMPB2)
      EQUIVALENCE   (CONST(61),K34)
      EQUIVALENCE
C
C
C
C
      EQUIVALENCE (TIME,T)
      MXDMP = 0
      IF (NFUNT .GT. TIME)   GO TO 25
C
C  evaluate piecewise linear functions of time
C
      CALL WASP8 (MFUNC,BFUNC,NFUNC,3,ITIMF,NFUNT,73)
      ITIMF = ITIMF + 1
 25   TEMP(1) = MFUNC(1) * (TIME-NFUNT) + BFUNC(1)
      TEMP(2) = MFUNC(2) * (TIME-NFUNT) + BFUNC(2)
      IAV     = MFUNC(3) * (TIME-NFUNT) + BFUNC(3)
      F       = MFUNC(4) * (TIME-NFUNT) + BFUNC(4)
      KE      = MFUNC(5) * (TIME-NFUNT) + BFUNC(5)
      WIND    = MFUNC(6) * (TIME-NFUNT) + BFUNC(6)
      IF (IDISK .EQ. 0 )    GO TO 50
      PTIME = TIME + 0.0001 * TIME
      WRITE (OUT,201) PTIME
C
C start main do loop
C
 50   DO 100 ISEG = 1,NOSEG
C                                        set concentrations for segment
      C1 = C(1,ISEG)
      C2 = C(2,ISEG)
      C3 = C(3,ISEG)
      C4 = C(4,ISEG)
      C5 = C(5,ISEG)
      C6 = C(6,ISEG)
      C7 = C(7,ISEG)
      C8 = C(8,ISEG)
      C9 = C(9,ISEG)
      C10= C(10,ISEG)
      C11= C(11,ISEG)
C
C   segment numbers less than thirteen (13) are surface segments and
```

```
C   segment numbers greater than thirteen (13) are bottom segments
C
      IF (ISEG .LT. 13) THEN
          TOPSEG = .TRUE.
       ELSE
          TOPSEG = .FALSE.
       ENDIF
      H = DEPTH(ISEG)
      VOL = BVOL(ISEG)
      IF (TOPSEG) THEN
          TEM = TEMP(1)
       ELSE
          TEM = TEMP(2)
       ENDIF
      TEMP20 = TEM - 20
C
C          ***************************
C          *   SYSTEM 1 - DIATOMS    *
C          ***************************
C
C evaluate saturated growth rate due to temperature
C
      IF(TEM .GT. 0.0 .AND.  TEM .LT. 30.0) THEN
         GMAXD = 0.10328*(TEM) + 0.0408
       ELSE
       IF (TEM .GT. 35) THEN
           GMAXD = 0.0
        ELSE
           GMAXD = -0.7647059*(TEM) + 26.73529
        ENDIF
       ENDIF
C
C  reduction in growth rate due to non-optimum light
C
      DSHD = (30.0 * C1)/ 3.281
      BGSHD = (30.0 * (C3+C4))/ 3.281
      KED = KE + DSHD + BGSHD
      IF (.NOT. TOPSEG) BIAV = IAV * EXP(-KED*PREVH)
      TEMP1 = KED * H
      IF (TOPSEG) THEN
          TEMP2 = IAV/ISD/F
       ELSE
          TEMP2 = BIAV/ISD/F
       ENDIF
      TEMP3 = EXP(-TEMP1)
      RD = 2.718 * F/ TEMP1 *(EXP(-TEMP2*TEMP3) - EXP(-TEMP2))
C
C  reduction due to non-optimum nutrients
C
C  nitrogen effect
C
      CN = C6 + C7
      NITD = CN / (CN + KMND)
C
```

```
C  phosphorus effect
C
      PHOSD = C9 / (C9 + KMPD)
C
C  salinity effect
C
      T1D = ALOG10(S1D)
      T2D = ALOG10(S2D)
      S   = ALOG10(C10)
      X   = 1.0 - MINPD
      IF (S .LE. T1D)   SALD = 1.0
      IF (S .GT. T1D .AND. S .LE. T2D) SALD = 1.0 - X*(S-T1D)
      IF (S .GT. T2D)   SALD = MINPD
C
C  total nutrient reduction effect
C
      NUTD = NITD * PHOSD * SALD
C
C  calculate diatom growth rate
C
      GRD = GMAXD * RD * NUTD
C
C  Diatom Death Rate - due to respiration and death
C
      RESP = KRD * KRTD**TEMP20
      DRD = RESP + KDRD
      SETLD = SVD * (VOL/H)*C1
C
C  calculate derivative
C
      IF (TOPSEG) THEN
          CD(1,ISEG) = (GRD-DRD)*C1*VOL - SETLD
          PREVD = SETLD
       ELSE
          CD(1,ISEG) =  (GRD-DRD)*C1*VOL + PREVD - SETLD
       ENDIF
C
C
C          ********************************
C          *  SYSTEM 2 - GREEN ALGAE      *
C          ********************************
C
C  evaluate saturated growth rate due to temp.
C
      IF (TEM.GT.0.0 .AND.  TEM.LT.35.0) THEN
          GMAXG = 0.1183085*(TEM) - 0.5954654
       ELSE
          GMAXG = -0.3587327*(TEM) + 16.12176
       ENDIF
C
C  reduction in growth rate due to non-optimum light
C
      GSHD = (30.0 *C2)/3.281
      BGSHD = (30.0*(C3+C4))/3.281
```

```
      KEG = KE + GSHD + BGSHD
      IF (.NOT. TOPSEG) BIAV = IAV * EXP(-KEG*PREVH)
      TEMP1 = KEG * H
      IF (TOPSEG) THEN
          TEMP2 = IAV/ISG/F
       ELSE
          TEMP2 = BIAV/ISG/F
       ENDIF
      TEMP3 = EXP(-TEMP1)
      RG = 2.718 * F/ TEMP1 * (EXP(-TEMP2*TEMP3) - EXP(-TEMP2))
C
C  reduction due to non-optimum nutrients
C
C  nitrogen effect
C
      CN = C6 + C7
      NITG = CN / (CN + KMNG)
C
C  phosphorus effect
C
      PHOSG = C9 / (C9 + KMPG)
C
C  salinity effect
C
      T1G = ALOG10(S1G)
      T2G = ALOG10(S2G)
      S   = ALOG10(C10)
      X   = 1.0 - MINPG
      IF (S.LE.T1G)     SALG = 1.0
      IF (S.GT.T1G .AND. S.LE.T2G)  SALG = 1.0 - X*(S-T1G)
      IF (S.GT.T2G)     SALG = MINPG
C
C  total nutrient reduction
C
      NUTG = NITG * PHOSG * SALG
C
C  calculate growth rate
C
      GRG = GMAXG * RG * NUTG
C
C  Green Death Rate - due to algal respiration and death
C
      RESP = KRG * KRTG**TEMP20
      DRG = RESP + KDRG
      SETLG = SVG * (VOL/H) *C2
C
C  calculate derivative
C
      IF (TOPSEG )  THEN
          CD(2,ISEG) =  (GRG-DRG)*C2*VOL - SETLG
          PREVG = SETLG
       ELSE
          CD(2,ISEG) =  (GRG-DRG)*C2*VOL + PREVG - SETLG
       ENDIF
```

```
C
C          ****************************************
C          *              SYSTEM 3                *
C          * NON-NITROGEN FIXING BLUE GREEN ALGAE  *
C          ****************************************
C
 773  FORMAT ('SYSTEM 3')
C  saturated growth rate due to temperature
C
      IF (TEM.GT.0.0 .AND. TEM.LE.13.0 )
      IF (TEM.GT.13.0 .AND. TEM.LE.25.0)
      IF (TEM.GT.25.0)   GMAXBG = 0.1711044*TEM - 2.4287643
C
C  reduction in growth rate due to non-optimum light
C
      BGSHD = (30.0 *(C3+C4))/3.281
      KEBG = KE + BGSHD
      IF (.NOT. TOPSEG)   BIAV = IAV * EXP(-KEBG*PREVH)
      TEMP1 = KEBG * H
      IF (TOPSEG) THEN
          TEMP2 = IAV/ISB1/F
       ELSE
          TEMP2 =BIAV/ISB1/F
       ENDIF
      TEMP3 = EXP(-TEMP1)
      RB1 = 2.718 * F/TEMP1 * (EXP(-TEMP2*TEMP3) - EXP(-TEMP2))
C     IF (TOPSEG) RB1=1.0
C
C  reduction due to non-optimum nutrients
C
C  nitrogen effect
C
      CN = C6 + C7
      NITB1 = CN / (CN + KMNB1)
C
C  phosphorous effect
C
      PHOSB1 = C9 / (C9 + KMPB1)
C
C  salinity effect
C
      T1B1 = ALOG10(S1B1)
      T2B1 = ALOG10(S2B1)
      S    = ALOG10(C10)
      X    = 1.0 - MINPB1
      IF (S .LE. T1B1)  SALB1 = 1.0
      IF (S .GT. T1B1 .AND. S .LE. T2B1) SALB1 = 1.0 - X*(S-T1B1)
      IF (S .GT. T2B1)  SALB1 = MINPB1
      NUTB1 = NITB1 * PHOSB1 * SALB1
C
C  calculate growth rate
C
      GRB1 = GMAXBG * RB1 * NUTB1
C
```

```
C  death rate
C
      RESP = KRB1 * KRTB1**TEMP20
      DRB1 = RESP + KDRB1
      SETLB1 = SVB1 * (VOL/H) * C3
      BUGSV = SVB1/H
C
C  calculate derivative
C
      IF (TOPSEG) THEN
          CD(3,ISEG) =  (GRB1-DRB1)*C3*VOL - SETLB1
          PREVB1 = SETLB1
       ELSE
          CD(3,ISEG) =  (GRB1-DRB1)*C3*VOL + PREVB1 - SETLB1
       ENDIF
C
C          ****************************************
C          *              SYSTEM 4                *
C          *     NITROGEN FIXING BLUE GREENS      *
C          ****************************************
C
 774  FORMAT ('SYSTEM 4')
C  saturated growth rate
C
      IF (TEM.GT.0.0 .AND. TEM.LE.13.0)
      IF (TEM.GT.13.0 .AND. TEM.LE.25.0)
      IF (TEM.GT.25.0)  GMAXBG = 0.1711044*(TEM) - 2.4287643
C
C  reduction in growth rate due to non-optmum light
C
      BGSHD = (30.0 * (C3+C4))/3.281
      KEBG = KE + BGSHD
      IF (.NOT. TOPSEG)  BIAV = IAV * EXP(-KEBG*PREVH)
      TEMP1 = KEBG * H
      IF (TOPSEG) THEN
          TEMP2 = IAV/ISB2/F
       ELSE
          TEMP2 = BIAV/ISB2/F
       ENDIF
      TEMP3 = EXP(-TEMP1)
      RB2 = 2.718 * F/ TEMP1*(EXP(-TEMP2*TEMP3)-EXP(-TEMP2))
C     IF (TOPSEG) RB2 = 1.0
C
C  reduction due to non-optimum nutrients
C
C  nitrogen effect  - (no limitation, fix nitrogen from atmosphere)
C
      NITB2 = 1.0
C
C  phosphorus effect
C
      PHOSB2 = C9 / (C9 + KMPB2)
C
C  salinity effect
```

```
C
      T1B2 = ALOG10(S1B2)
      T2B2 = ALOG10(S2B2)
      S    = ALOG10(C10)
      X    = 1.0 - MINPB2
      IF (S .LE. T1B2)  SALB2 = 1.0
      IF (S .GT. T1B2 .AND. S .LE. T2B2) SALB2 = 1.0 - X*(S-T1B2)
      IF (S .GT. T2B2)  SALB2 = MINPB2
      NUTB2 = NITB2 * PHOSB2 * SALB2
C
C  growth rate
C
      GRB2 = GMAXBG * RB2 * NUTB2
C
C  death rate
C
      RESP = KRB2 * KRTB2**TEMP20
      DRB2 = RESP + KDRB2
      SETLB2 = SVB2 * (VOL/H) * C4
C
C  calculate derivative
C
      IF (TOPSEG) THEN
          CD(4,ISEG) =  (GRB2-DRB2)*C4*VOL - SETLB2
          PREVB2 = SETLB2
       ELSE
          CD(4,ISEG) =  (GRB2-DRB2)*C4*VOL + PREVB2 - SETLB2
       ENDIF
C
C         ************************************
C         *   SYSTEM 5 - ORGANIC NITROGEN    *
C         ************************************
C
 775  FORMAT ('SYSTEM 5')
C  source due to phytoplankton endogenous respiration
C
C  nchlb2 is written throughout as nchlb1
C
      SR5D = NCHLD * DRD * C1* (1.0-DEADD)
      SR5G = NCHLG * DRG * C2 * (1.0 - DEADG)
      SR5B1 = NCHLB1 * DRB1 * C3 * (1.0 - DEADB1)
      SR5B2 = NCHLB1 * DRB2 * C4 * (1.0 - DEADB2)
      SR5 = SR5D + SR5G + SR5B1 + SR5B2
C
C  sink due to ammonification (org.N - NH3)
C
      SK5 = (K34 * K34T**TEMP20) * C5
C
C  amount of nitrogen in the system
C
      TON = (NCHLD*C1) + (NCHLG*C2) + (NCHLB1*C3) + (NCHLB1*C4) + C5
      TN = TON + C6 + C7
      TIN = C6 + C7
C
```

```
C  calculate derivative
C
      CD(5,ISEG) =  (SR5 - SK5)*VOL
C
C          ************************************
C          *       SYSTEM 6 - AMMONIA         *
C          ************************************
C
 776  FORMAT ('SYSTEM 6')
C  source due to ammonification (org.N - NH3)
C
      SR6 = SK5
C
C  sink of NH3 due to nitrification
C
      SK61 = (K45 * K45T**TEMP20) * C6
C
C  sink due to phytoplankton uptake
C
      PNH3D = C6 * C7/((KMND+C6)*(KMND+C7))
      SK62D = (GRD * C1) * PNH3D * NCHLD
      PNH3G = C6*C7/((KMNG+C6)*(KMNG+C7)) + C6*KMNG/((C6+C7)*(KMNG+C7))
      SK62G = (GRG*C2) * PNH3G * NCHLG
      PNH3B1= C6*C7/((KMNB1+C6)*(KMNB1+C7))
      SK62B1= (GRB1*C3) * PNH3B1 * NCHLB1
      SK62B2 = 0.0
      SK62 = SK62D + SK62G + SK62B1 + SK62B2
C
C  calculate derivative
C
      CD(6,ISEG) =  (SR6 - SK61 - SK62)*VOL
C
C
C          ************************************
C          *     SYSTEM 7 - NO2+NO3           *
C          ************************************
C
 777  FORMAT ('SYSTEM 7')
C  source due to nitrification
C
      SR7 = SK61
C
C  sink due to phytoplankton uptake
C
      SK7D = (1.0 - PNH3D) * NCHLD * (GRD*C1)
      SK7G = (1.0 - PNH3G) * NCHLG * (GRG*C2)
      SK7B1= (1.0 - PNH3B1) * NCHLB1 * (GRB1*C3)
      SK7B2 = 0.0
      SK7 = SK7D + SK7G + SK7B1 + SK7B2
C
C  calculate derivative
C
      CD(7,ISEG) =  (SR7 - SK7)*VOL
C
```

```
C
C          ************************************
C          *  SYSTEM 8 - ORGANIC PHOSPHORUS   *
C          ************************************
C
 778  FORMAT ('SYSTEM 8')
C  sink due to ortho-p transformation (mineralization)
C
      SK8 = (K67 * K67T**TEMP20) * C8
C
C  source due to  phytoplankton endogenous respiration
C
      SR8D = PCHLD / NCHLD * SR5D
      SR8G = PCHLG / NCHLG * SR5G
      SR8B1 = PCHLB1 / NCHLB1 * SR5B1
C   nchlb1=nchlb2 and was changed here for temporary simplicity
C
      SR8B2 = PCHLB2 / NCHLB1 * SR5B2
      SR8 = SR8D + SR8G + SR8B1 + SR8B2
C
C  amount of phosphorus in the system
C
      TOP = C8 + (PCHLD*C1) + (PCHLG*C2) + (PCHLB1*C3) + (PCHLB2*C4)
      TP  = TOP + C9
C
C  calculate derivative
C
      CD(8,ISEG) =  (SR8 - SK8)*VOL
C
C          ************************************
C          *     SYSTEM  9 - ORTHO-P          *
C          ************************************
C
 779  FORMAT ('SYSTEM 9')
C  source due to mineralization (P-PO4)
C
      SR9 = SK8
C
C  sink due to phytoplankton uptake
C
      SK9D = PCHLD * (GRD*C1)
      SK9G = PCHLG * (GRG*C2)
      SK9B1 = PCHLB1 * (GRB1*C3)
      SK9B2 = PCHLB2 * (GRB2*C4)
      SK9 = SK9D + SK9G + SK9B1 + SK9B2
C
C  calculate derivative
C
      CD(9,ISEG) =  (SR9 - SK9)*VOL
C
C          ********************************
C          *     SYSTEM 10 - SALINITY     *
C          ********************************
C
```

```
 780  FORMAT ('SYSTEM 10')
      CD(10,ISEG) = 0.0
C
C          **********************************
C          *  SYSTEM 11 - DISSOLVED OXYGEN  *
C          **********************************
C
 781  FORMAT ('SYSTEM 11')
C  sink due to phytoplankton uptake
C
      SK11D = (KRD * KRTD**TEMP20) * OCHLD * C1
      SK11G = (KRG * KRTG**TEMP20) * OCHLG * C2
      SK11B1 = (KRB1 * KRTB1**TEMP20) * OCHLB1 * C3
      SK11B2 = (KRB2 * KRTB2**TEMP20) * OCHLB2 * C3
      SK111 = SK11D + SK11G + SK11B1 +SK11B2
C
C  sink due to oxygen needed for nitrification
C
      SK112 = 4.57 * SK61
C
C  sink due to benthic demand
C
      IF (.NOT. TOPSEG) THEN
          KBNTH = KBN20 * 1.028**TEMP20
          SK113 = KBNTH * 3.281/H
       ELSE
          SK113 = 0.0
       ENDIF
C
C  oxygen production by phytoplankton
C
      SR11D = (GRD*C1) * OCHLD
      SR11G = (GRG*C2) * OCHLG
      SR11B1 = (GRB1*C3) * OCHLB1
      SR11B2 = (GRB2*C4) * OCHLB2
      SR111 = SR11D + SR11G + SR11B1 + SR11B2
C
C  source due to reaeration
C
      KA20 =12.9* VELSG(ISEG)**0.5 / H**1.5 + 0.4 * WIND/H
      KA = KA20 * 1.028**TEMP20
      CS = 14.6244 - 0.367134*TEM + 0.0044972*TEM*TEM - 0.0966*C10
      SR112 = (CS -C11) * KA
      IF (.NOT. TOPSEG) SR112 = 0.0
C
C  calculate derivative
C
      CD(11,ISEG) =  (SR111+ SR112- SK111- SK112- SK113)*VOL
      PREVH = H
C  print the results
C
      IF (IDISK .EQ.1)
      IF (IDISK.EQ.1.AND.ISEG.EQ.7)
      IF (IDISK.EQ.1.AND.ISEG.EQ.8)
```

```
C     IF (IDISK.EQ.1.AND.ISEG.EQ.9)
C    .  WRITE(8,205) PTIME,C6,C7,C9,C10,(C1+C2+C3+C4)*1000,C11
      IF (IDISK.EQ.1.AND.ISEG.EQ.10)
C     IF (IDISK.EQ.1.AND.ISEG.EQ.11)
C    .  WRITE(81,205) PTIME,C6,C7,C9,C10,(C1+C2+C3+C4)*1000,C11
      IF (IDISK.EQ.1.AND.ISEG.EQ.12)
      IF (IDISK.EQ.1.AND.ISEG.EQ.7) WRITE(83,206) PTIME,C1,C2,C3,C4
      IF (IDISK.EQ.1.AND.ISEG.EQ.8) WRITE(84,206) PTIME,C1,C2,C3,C4
C     IF (IDISK.EQ.1.AND.ISEG.EQ.9) WRITE(85,206) PTIME,C1,C2,C3,C4
      IF (IDISK.EQ.1.AND.ISEG.EQ.10) WRITE(86,206) PTIME,C1,C2,C3,C4
      IF (IDISK.EQ.1.AND.ISEG.EQ.11) WRITE(87,206) PTIME,C1,C2,C3,C4
      IF (IDISK.EQ.1.AND.ISEG.EQ.12)WRITE(88,206) PTIME,C1,C2,C3,C4
      IF (IDISK.EQ.1.AND.ISEG.EQ.7) WRITE(81,207)
C     IF (IDISK.EQ.1.AND.ISEG.EQ.9)
C    .   WRITE(83,207) PTIME,RB1,NITB1,PHOSB1,SALB1,GRB1,DRB1,BUGSV
C     IF (IDISK.EQ.1.AND.ISEG.EQ.11)
C    .  WRITE(84,207) PTIME,RB1,NITB1,PHOSB1,SALB1,GRB1,DRB1,BUGSV
      IF (IDISK.EQ.1.AND.ISEG.EQ.12)
  100 CONTINUE
  201 FORMAT (5X,F10.3)
  203 FORMAT (1X,F9.3,11E9.3)
  204 FORMAT (10F9.2)
  205 FORMAT (7F10.4)
  206 FORMAT (5F10.4)
  207 FORMAT (8F10.4)
      IDISK = 0
      RETURN
      END
```

UNIVERSITY OF VIRGINIA
School of Engineering and Applied Science

The University of Virginia's School of Engineering and Applied Science has an undergraduate enrollment of approximately 1,500 students with a graduate enrollment of approximately 560. There are 150 faculty members, a majority of whom conduct research in addition to teaching.

Research is a vital part of the educational program and interests parallel academic specialties. These range from the classical engineering disciplines of Chemical, Civil, Electrical, and Mechanical and Aerospace to newer, more specialized fields of Biomedical Engineering, Systems Engineering, Materials Science, Nuclear Engineering and Engineering Physics, Applied Mathematics and Computer Science. Within these disciplines there are well equipped laboratories for conducting highly specialized research. All departments offer the doctorate; Biomedical and Materials Science grant only graduate degrees. In addition, courses in the humanities are offered within the School.

The University of Virginia (which includes approximately 2,000 faculty and a total of full-time student enrollment of about 16,400), also offers professional degrees under the schools of Architecture, Law, Medicine, Nursing, Commerce, Business Administration, and Education. In addition, the College of Arts and Sciences houses departments of Mathematics, Physics, Chemistry and others relevant to the engineering research program. The School of Engineering and Applied Science is an integral part of this University community which provides opportunities for interdisciplinary work in pursuit of the basic goals of education, research, and public service.